

AWARD NUMBER: **W81XWH-13-1-0122**

TITLE: **Potential of Targeting PDE1C/2A for Suppressing Metastatic Ovarian Cancers**

PRINCIPAL INVESTIGATOR: Shuang Huang

CONTRACTING ORGANIZATION: Georgia Regents University
Augusta, GA 30912

REPORT DATE: September 2015

TYPE OF REPORT: Final

PREPARED FOR: U.S. Army Medical Research and Materiel Command
Fort Detrick, Maryland 21702-5012

DISTRIBUTION STATEMENT: Approved for Public Release;
Distribution Unlimited

The views, opinions and/or findings contained in this report are those of the author(s) and should not be construed as an official Department of the Army position, policy or decision unless so designated by other documentation.

REPORT DOCUMENTATION PAGE			<i>Form Approved</i> <i>OMB No. 0704-0188</i>		
Public reporting burden for this collection of information is estimated to average 1 hour per response, including the time for reviewing instructions, searching existing data sources, gathering and maintaining the data needed, and completing and reviewing this collection of information. Send comments regarding this burden estimate or any other aspect of this collection of information, including suggestions for reducing this burden to Department of Defense, Washington Headquarters Services, Directorate for Information Operations and Reports (0704-0188), 1215 Jefferson Davis Highway, Suite 1204, Arlington, VA 22202-4302. Respondents should be aware that notwithstanding any other provision of law, no person shall be subject to any penalty for failing to comply with a collection of information if it does not display a currently valid OMB control number. PLEASE DO NOT RETURN YOUR FORM TO THE ABOVE ADDRESS.					
1. REPORT DATE September 2015		2. REPORT TYPE Final		3. DATES COVERED 06/15/2013 -06/14/2015	
4. TITLE AND SUBTITLE Potential of Targeting PDE1C/2A for Suppressing Metastatic Ovarian Cancers				5a. CONTRACT NUMBER	
				5b. GRANT NUMBER W81XWH-13-1-0122	
				5c. PROGRAM ELEMENT NUMBER	
6. AUTHOR(S) Shuang Huang E-Mail: shuanghuang@ufl.edu				5d. PROJECT NUMBER	
				5e. TASK NUMBER	
				5f. WORK UNIT NUMBER	
7. PERFORMING ORGANIZATION NAME(S) AND ADDRESS(ES) Georgia Regents University Augusta, GA				8. PERFORMING ORGANIZATION REPORT NUMBER	
9. SPONSORING / MONITORING AGENCY NAME(S) AND ADDRESS(ES) U.S. Army Medical Research and Materiel Command Fort Detrick, Maryland 21702-5012				10. SPONSOR/MONITOR'S ACRONYM(S)	
				11. SPONSOR/MONITOR'S REPORT NUMBER(S)	
12. DISTRIBUTION / AVAILABILITY STATEMENT Approved for Public Release; Distribution Unlimited					
13. SUPPLEMENTARY NOTES					
14. ABSTRACT ERK signaling pathway has long been suggested as a therapeutic target for ovarian cancer progression and metastasis. In our previous studies, we showed that 1) high Erk activity is sensitive to the elevation of intracellular cAMP concentration; and 2) agents elevating cellular cAMP suppresses growth of aggressive ovarian cancer cells. This proposal is sought to 1) understand molecular mechanisms associated with forskolin/PDE2 inhibitor-induced apoptosis of aggressive ovarian cancer cells and 2) to evaluate the translation value of treating aggressive ovarian cancer cells with forskolin and PDE2 inhibitor in an intraperitoneal xenograft model. In first year of the funding, we showed that knockdown of PDE2A rendered ovarian cancer cells susceptible for forskolin-induced cell growth inhibition/apoptosis. We further showed that combined use of forskolin and Bay60-7550 (PDE2 inhibitor) downregulates the levels of Bcl2, survivin and phosphorylated Akt whereas induces the expression of Bim1. The effect of forskolin/Bay60-7550 is clearly mediated by PKA because PKA inhibitor H89 abolished growth inhibition caused by forskolin/Bay60-7550. In second year of the funding, we evaluated the potential of using cocktail of forskolin and Bay60-7550 to suppress ovarian tumor development. We found that such cocktail is safe to the recipient mice and can effectively slow intraperitoneal metastatic colonization of ovary tumors. We believe that results from our study have built a solid basis for further testing such cocktail in clinic.					
15. SUBJECT TERMS Nothing listed					
16. SECURITY CLASSIFICATION OF:			17. LIMITATION OF ABSTRACT	18. NUMBER OF PAGES	19a. NAME OF RESPONSIBLE PERSON
a. REPORT	b. ABSTRACT	c. THIS PAGE			USAMRMC
U	U	U	UU	38	19b. TELEPHONE NUMBER (include area code)

Table of Contents

	Page
1. Introduction.....	4
2. Keywords.....	5
3. Accomplishments.....	6
4. Impact.....	10
5. Changes/Problems.....	11
6. Products.....	12
7. Participants & Other Collaborating Organizations.....	13
8. Special Reporting Requirements.....	N/A
9. Appendices.....	

Introduction

Ovarian cancer has the highest mortality rate among gynecological cancers. Due to the lack of symptoms with early stage disease and no effective screening strategies, ovarian tumors have become metastatic at the time of clinical diagnosis in 75% of ovarian cancer patients. Unfortunately, advances in surgical techniques and chemotherapy have not significantly improved the survival of ovarian cancer patients in past several decades. Therefore, the novel therapeutic approaches are urgently needed for treating metastatic ovarian cancers.

ERK signaling pathway plays a critical role in the survival and proliferation of ovarian cancer cells. It is thus expected that approaches interfering with ERK signaling pathway will lead to the suppression of ovarian cancer progression and metastasis. In our previous studies, we showed that 1) Erk activity is higher in aggressive ovarian cancer cells and is required for their survival; 2) high Erk activity is sensitive to the elevation of intracellular cAMP concentration; 3) combined use of forskolin and PDE2 inhibitor induces apoptosis of aggressive ovarian cancer cells. This proposal is 1) sought to understand molecular mechanisms associated with forskolin/PDE2 inhibitor-induced apoptosis of aggressive ovarian cancer cells and 2) to evaluate the translation value of treating aggressive ovarian cancer cells with forskolin and PDE2 inhibitor in an intraperitoneal xenograft model. In first year of the funding, we showed that knockdown of PDE2A rendered ovarian cancer cells susceptible for forskolin-induced cell growth inhibition/apoptosis. We further showed that combined use of forskolin and Bay60-7550 (PDE2 inhibitor) downregulates the levels of Bcl2, survivin and phosphorylated Akt whereas induces the expression of Bim1. The effect of forskolin/Bay60-7550 is clearly mediated by PKA because PKA inhibitor H89 abolished growth inhibition caused by forskolin/Bay60-7550. These finding thus laid the foundation to test the efficacy of combined use of forskolin and Bay60-7550 to treat ovarian cancer in second year of the funding. With the aid of well-established metastatic ovarian cancer implantation model, we showed that cocktail of forskolin and Bay60-7550 greatly inhibited tumor outgrowth and improved survival of mice bearing with ovary tumors. In conclusion, our study provides an ovarian cancer-targeted therapeutic strategy with clinically available forskolin and PDE2A inhibitor.

Keywords

Ovarian cancer, metastasis, PDE, cAMP, ERK, apoptosis, cell growth, tumor progression, cell survival

Accomplishments

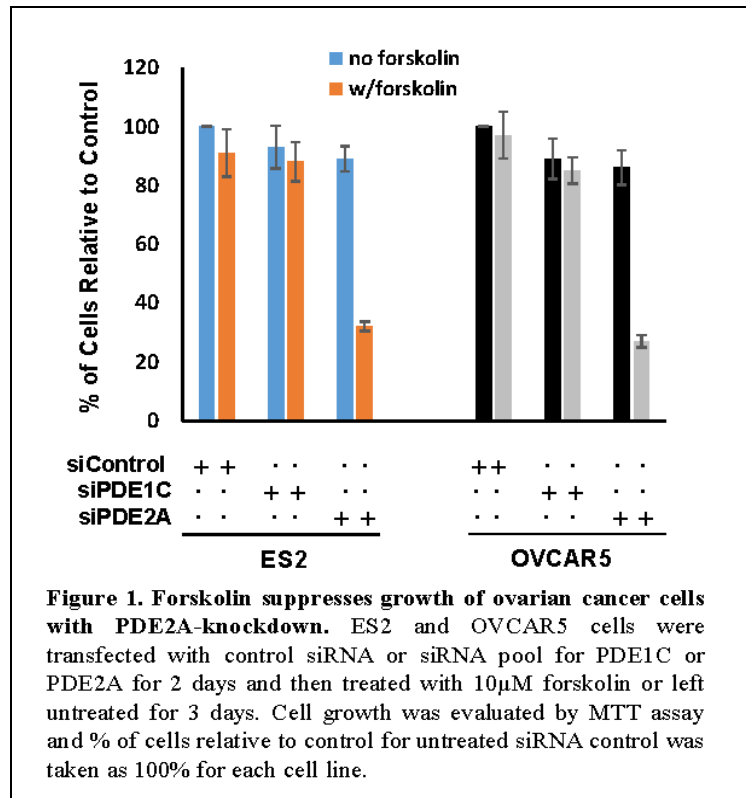
1. What were the major goals of the project?

There are two major goals in approved SOW: 1) **Elucidate molecular mechanisms associated with PDE1/2 inhibitors-induced apoptosis of metastatic OCCs** (completed in first year of the funding period). 2) **Evaluate the translation value of using PDE1/2 inhibitors to suppress ovarian cancer metastasis** (completed in second year of the funding period).

2. What was accomplished under these goals?

The major tasks in the first year of this proposal are 1) Examine the effect of PDE1C and PDE2A-specific siRNAs on ovarian cancer cell growth inhibition/apoptosis (months 1-4); 2) Examine the effect of PDE1 and PDE2 inhibitors (8-methoxymethyl-IBMX and Bay60-7550) on ovarian cancer cell growth inhibition/apoptosis (months 5-8); 3) Determine potential involvement of PKA in PDE1/2 inhibitor-led ovarian cancer cell growth inhibition/apoptosis.

Task 1: We introduced PDE1C or PDE2A siRNAs into ovarian cancer ES2 and OVCAR5 cells



and measured their effect on cell growth. Only slightly growth inhibitory effect was seen with PDE2A siRNA in aggressive ovarian cancer cells. To determine if lack of growth inhibition by PDE siRNA is caused by poor accumulation of cellular cAMP in these cells, we treated these cells with 10 μ M forskolin two days after siRNA transfection. MTT assay showed that forskolin suppressed over 60% of cell growth in cells with PDE2A-knockdown but not PDE1C-knockdown in 3-day growth period. Silencing both PDE1C and PDE2A did not make forskolin more growth inhibitory. Moreover, forskolin alone only marginally inhibited growth of cells treated with control siRNA (Fig.1). Similar results were also generated with another four ovarian

cancer cells lines (HEY, OCC1, OVCAR8 and SK-OV3) (data not shown). These results suggest that forskolin can effectively ovarian cancer cells growth when PDE2A is blocked.

Task 2: ES2 and OVCAR5 cells were first treated with PDE2 inhibitor Bay60-7550 or PDE1 inhibitor 8-methoxymethyl-IBMX for 2 h followed by treatment of forskolin for 3 days. MTT assay clearly showed that Bay60-7550, but not 8-methoxymethyl-IBMX rendered cells responding to forskolin for growth inhibition (Fig.2A). Similar results were also generated with HEY, OCC1, OVCAR8 and SK-OV3 cells (data not shown). To determine whether growth inhibition was caused by cell death, we performed Annexin V/PI-staining on OVCAR5 cells

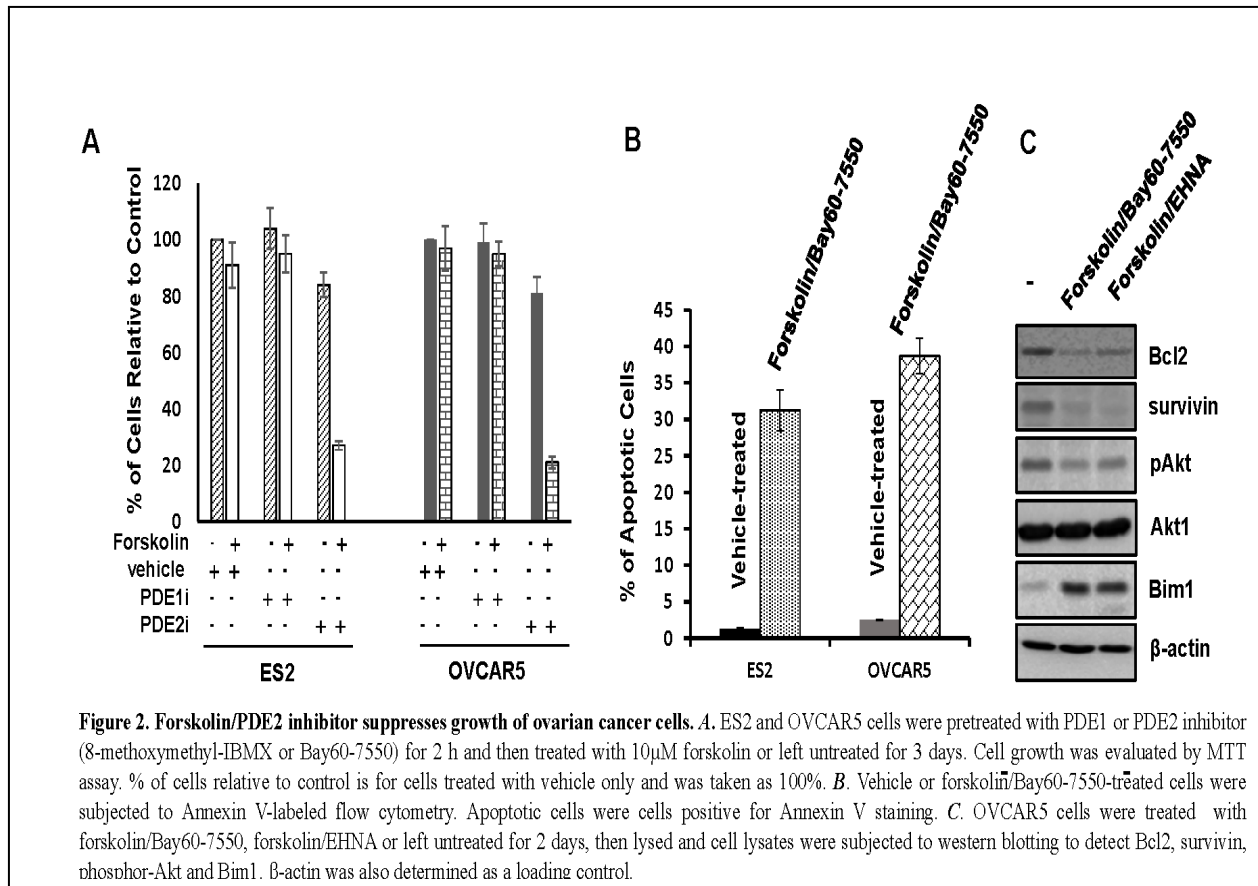


Figure 2. Forskolin/PDE2 inhibitor suppresses growth of ovarian cancer cells. A. ES2 and OVCAR5 cells were pretreated with PDE1 or PDE2 inhibitor (8-methoxymethyl-IBMX or Bay60-7550) for 2 h and then treated with 10 μ M forskolin or left untreated for 3 days. Cell growth was evaluated by MTT assay. % of cells relative to control is for cells treated with vehicle only and was taken as 100%. B. Vehicle or forskolin/Bay60-7550-treated cells were subjected to Annexin V-labeled flow cytometry. Apoptotic cells were cells positive for Annexin V staining. C. OVCAR5 cells were treated with forskolin/Bay60-7550, forskolin/EHNA or left untreated for 2 days, then lysed and cell lysates were subjected to western blotting to detect Bcl2, survivin, phosphor-Akt and Bim1. β -actin was also determined as a loading control.

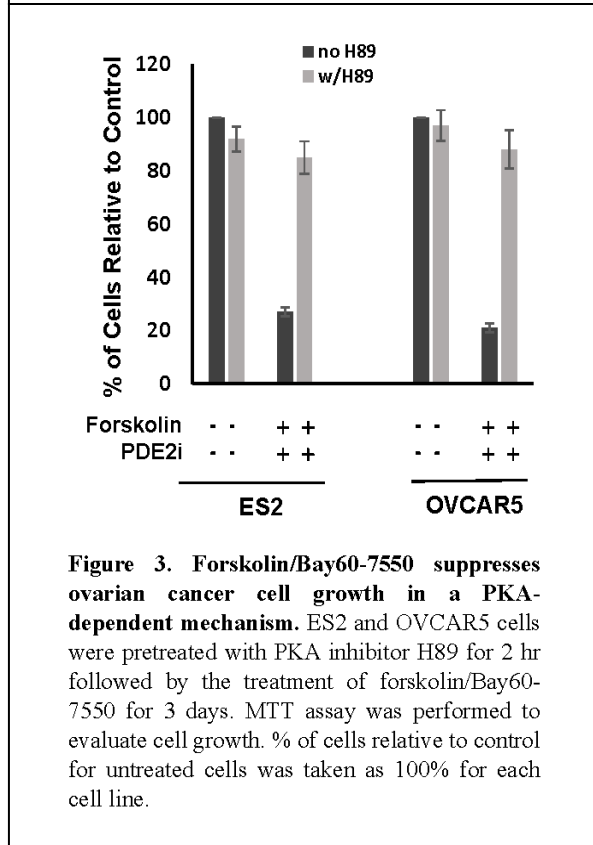


Figure 3. Forskolin/Bay60-7550 suppresses ovarian cancer cell growth in a PKA-dependent mechanism. ES2 and OVCAR5 cells were pretreated with PKA inhibitor H89 for 2 hr followed by the treatment of forskolin/Bay60-7550 for 3 days. MTT assay was performed to evaluate cell growth. % of cells relative to control for untreated cells was taken as 100% for each cell line.

treated with or without forskolin/Bay60-7550. Flow cytometry revealed a dramatic increase in apoptotic cells (Fig.2B). To elucidate molecular mechanism associated with forskolin/PDE2 inhibitor-induced apoptosis, we collected cell lysates from untreated OVCAR5 cells and OVCAR5 cells treated with forskolin/Bay60-7550 or forskolin/EHNA (another PDE2 inhibitor). Western blotting showed combined treatment but none of them alone led to reduction in the abundance of Bcl2, survivin and phosphor-Akt while increased the level of Bim1 (Fig.2C). These results suggest that forskolin/PDE2 inhibitor treatment suppresses ovarian cancer cell growth by inducing cell death through the inhibition of Bcl2/survivin/phosphor-Akt/and upregulation of Bim1.

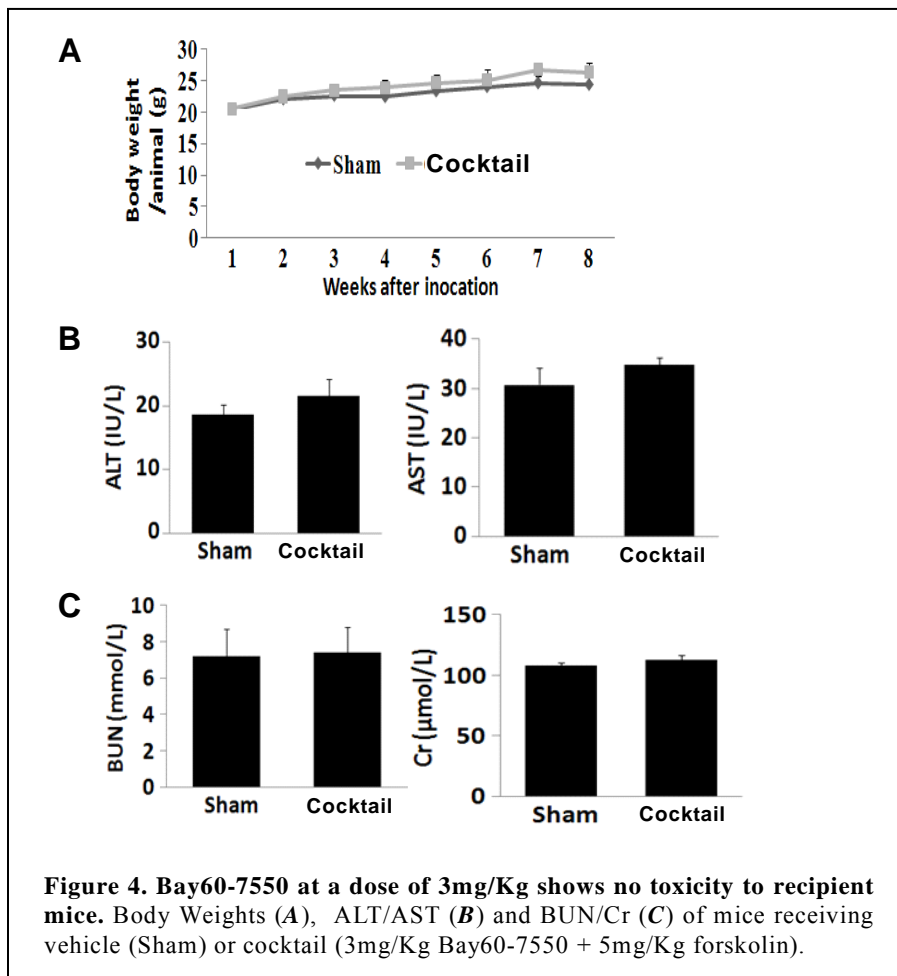
Task 3: To determine the potential role of PKA in forskolin/Bay60-7550-led ovarian cancer cell growth inhibition/apoptosis, we pretreated ES2 and OVCAR5 cells with PKA inhibitor H89 for

2 h prior to the treatment of forskolin/Bay60-7550. MTT assay showed that H89 abolished at least 80% of forskolin/Bay60-7550-caused growth inhibition (Fig.3), thus confirming that PKA as the mediator for forskolin/Bay60-7550-led growth inhibitory effect in ovarian cancer cells.

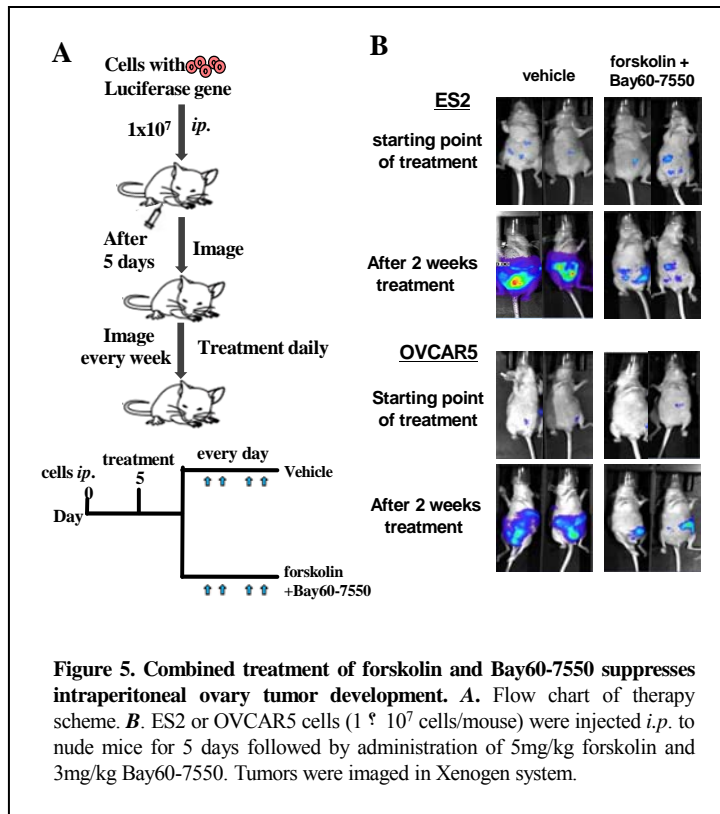
The major tasks in the second year of this proposal are 1) Pharmacokinetics studies of Bay60-7550 (months 13-14); 2) Toxicity Studies of Bay60-7550 (months 15-16); 3) Effect of Bay60-7550 on ovarian tumor cell metastatic colonization (17-24).

Task 4: Studies performed in year 1 of funding period showed that PDE2A inhibitor Bay60-7550 with forskolin was sufficient to suppress ovarian cancer cell growth. We thus performed pharmacokinetics studies with Bay60-7550 in mice. We intraperitoneally injected mice with Bay60-7550 at the dose of 1, 3, 10 and 30mg/kg and blood samples were collected via terminal heart puncture at 12 and 24 h followed by examining the amount of Bay60-7550 in blood with the aid of HPLC. While dose of 30mg/Kg was not tolerable to mice, dose above 3mg/Kg was sufficient to reach $> 1\mu\text{M}$ of drug concentration in the plasma after 24 h, a concentration equivalent to 10X effective concentration in *in vitro* settings. Therefore, a dose of 3mg/Kg was used for *in vivo* treatment experiments.

Task 5: The toxicity of Bay60-7550 was evaluated by determining various aspects. 1) We checked weigh loss by weighing animals daily in an eight-week period and did not notice



apparent difference between mice receiving vehicle (ethanol) and 3mg/Kg Bay60-7550/5mg/Kg forskolin (Fig.4A). 2) In the entire eight-week treatment period, we did not observe change in appetite or appearance of pre-death behavior such as pale skin and cachexia in mice receiving Bay60-7550/forskolin. 3) Level of GOT and GPT in serum did not indicate liver toxicity in mice receiving Bay60-7550/forskolin (Fig.4B). 4) Levels of Cr and BUN in serum also did not indicate any kidney toxicity in mice receiving Bay60-7550/forskolin (Fig.4C).



Task 6: To determine the effect of combined forskolin and Bay60-7550 treatment on ovary tumor development, female athymic nude mice were intraperitoneally injected with luciferase-expressing ES2 and OVCAR5 cells for 5 days followed by intraperitoneally administering vehicle or 5mg/Kg forskolin/3mg/Kg Bay60-7550 to animals (Fig.5A). Bioluminescence imaging showed that intraperitoneal xenografts could be detected 5 days after either ES2 or OVCAR5 cell injection (Fig.5B). Tumors propagated rapidly in mice receiving vehicle (Fig.5B). However, administering forskolin/Bay60-7550 deterred tumor propagation (Fig.5B). These results suggest that cocktail of forskolin and Bay60-7550 is effective in suppressing intraperitoneal ovary tumor development.

3. What opportunity from training and professional development has project provided?

Nothing to report.

4. How were the results disseminated to communities of interest?

Results were disseminated through publication in peer-reviewed scientific journals and poster presentations in University's Research Day.

5. What do you plan to do during the next reporting period to accomplish the goals?

Nothing to report.

Impact

1. What was the impact on the development of the discipline(s) of the project?

We found that simultaneously inducing the production of cAMP and blocking PDE2 activity suppress ovarian cancer progression and metastasis. Forskolin is a safe natural substance and PDE2 inhibitors (Bay60-7550) have been proven to be safe in clinic. Our findings lay the foundation to test the effectiveness of forskolin/Bay60-7550 to treat advanced ovarian cancer in clinic.

2. What was the impact on other disciplines?

Nothing to report.

3. What was the impact on technology transfer?

Nothing to report.

4. What was the impact on society beyond science and technology?

Nothing to report.

Changes/Problems

Nothing to report

Products

Publications

Yang L, Fang D, Chen H, Lu Y-Y, Dong Z, Ding H-F, Jing Q, Su S-B, and **Huang S.** (2015). Cyclin-dependent kinase 2 is an ideal target for ovary tumors with elevated cyclin E1 expression. *Oncotarget*, 6:20801-20812.

Fang D, Chen H, Zhu JY, Wang W, Teng Y, Ding H-F, Jing Q, Su S-B, and **Huang S.** (2016). Epithelial-Mesenchymal Transition of Ovarian Cancer Cells Is Sustained by Rac1 through Simultaneous Activation of MEK1/2 and Src Signaling Pathways. *Oncogene*, published on line (September, 2016).

Another two manuscripts are currently under revision or review.

Participants & Other Collaborating Organizations

1. What individuals have worked on the project?

No change

2. Has there been a change in the active other support of the PD/PI(s) or senior/key personnel since the last reporting period?

Nothing to report

3. What other organizations were involved as partners?

Nothing to report.

Cyclin-dependent kinase 2 is an ideal target for ovary tumors with elevated cyclin E1 expression

Liu Yang¹, Dongdong Fang¹, Huijun Chen², Yiyu Lu¹, Zheng Dong³, Han-Fei Ding⁴, Qing Jing⁵, Shi-Bing Su^{1,6} and Shuang Huang^{1,6,7}

¹ Research Center for Traditional Chinese Medicine Complexity System, Shanghai University of Traditional Chinese Medicine, Shanghai, China

² Department of Obstetrics and Gynecology, Zhongnan Hospital of Wuhan University, Wuhan, Hubei Province, China

³ Department of Anatomy and Cell Biology, Medical College of Georgia, Georgia Regents University, Augusta, GA, USA

⁴ Cancer Center, Georgia Regents University, Augusta, GA, USA

⁵ Department of Cardiology, Changhai Hospital, Shanghai, China

⁶ E-institute of Shanghai Municipal Education Committee, Shanghai University of Traditional Chinese Medicine, Shanghai, China

⁷ Department of Biochemistry and Molecular Biology, Medical College of Georgia, Georgia Regents University, Augusta, GA, USA

Correspondence to: Shuang Huang, **email:** shuang@gru.edu

Shi-Bing Su, **email:** shibingsu07@163.com

Keywords: CCNE1, Cdk2, ovarian cancer, tumor development

Received: April 01, 2015

Accepted: June 12, 2015

Published: June 23, 2015

This is an open-access article distributed under the terms of the Creative Commons Attribution License, which permits unrestricted use, distribution, and reproduction in any medium, provided the original author and source are credited.

ABSTRACT

CCNE1 gene amplification is present in 15-20% ovary tumor specimens. Here, we showed that Cyclin E1 (CCNE1) was overexpressed in 30% of established ovarian cancer cell lines. We also showed that CCNE1 was stained positive in over 40% of primary ovary tumor specimens regardless of their histological types while CCNE1 staining was either negative or low in normal ovary and benign ovary tumor tissues. However, the status of CCNE1 overexpression was not associated with the tumorigenic potential of ovarian cancer cell lines and also did not correlate with pathological grades of ovary tumor specimens. Subsequent experiments with CCNE1 siRNAs showed that knockdown of CCNE1 reduced cell growth only in cells with inherent CCNE1 overexpression, indicating that these cells may have developed an addiction to CCNE1 for growth/survival. As CCNE1 is a regulatory factor of cyclin-dependent kinase 2 (Cdk2), we investigated the effect of Cdk2 inhibitor on ovary tumorigenicity. Ovarian cancer cells with elevated CCNE1 expression were 40 times more sensitive to Cdk2 inhibitor SNS-032 than those without inherent CCNE1 overexpression. Moreover, SNS-032 greatly prolonged the survival of mice bearing ovary tumors with inherent CCNE1 overexpression. This study suggests that ovary tumors with elevated CCNE1 expression may be staged for Cdk2-targeted therapy.

INTRODUCTION

Ovarian cancer is the most deadly gynecological malignancy in women, largely due to late diagnosis as tumors have disseminated beyond the ovaries at the diagnosis in over 70% of ovarian cancer patients. In these cases, debulking with chemotherapy is the standard treatment procedure and yields a response rate of more

than 80%. However, almost all patients relapse and this clearly highlights the necessity to develop drugs useful for recurrent diseases [1].

Recent studies including The Cancer Genome Atlas (TCGA) reveal that ovarian cancers, especially high grade serous ovarian cancers (HGSOC), are marked by profound chromosomal aberrations (gene amplification and loss) rather than recurrent somatic mutations [2-4].

Besides near-ubiquitous TP53 mutation, point mutations are relatively uncommon at least in HGSOC [4]. Instead, HGSOCs contain widespread DNA copy number changes and one of the most frequent gene amplifications is *CCNE1* which occurs in at least 20% of HGSOC [2, 5, 6]. Importantly, *CCNE1* gene amplification correlates with CCNE1 overexpression in ovarian cancer and appear to have poorer disease-free and overall survival [6]. Immunohistochemistry studies with both primary and metastatic ovary tumor specimens further show that the abundance of cyclin E1 (CCNE1) correlates with tumor progression and predicts a poor prognosis in ovarian cancer patients [7-10]. Taken together, these findings highlight the importance of CCNE1 in ovary tumorigenesis.

CCNE1 mainly coordinates with Cdk2 to facilitate G1/S progression of cell cycle [11]. In ovarian cancer cells, enforcing CCNE1 expression stimulates cell proliferation [6] and increases colony formation [12]. *CCNE1* gene amplification-associated CCNE1 overexpression has been linked to the development of chemo-resistance in ovarian cancer [13, 14]. A recent study further shows that CCNE1 deregulation occurs early in fallopian tube secretory epithelial cell (FTSEC) transformation which promotes the formation of HGSOC [15]. Although all these findings implicate CCNE1 as a promising therapeutic target for at least the set of ovary tumors with elevated CCNE1 expression, developing small molecules to target CCNE1 directly is unlikely because CCNE1 acts as a regulatory subunit of cyclin-dependent kinase (Cdk) complex rather than as an enzyme or receptor. As ovary tumors with elevated CCNE1 level often exhibit higher Cdk2 expression [5, 15] and most of CCNE1-associated tumor promoting effects require the participation of Cdk2 [16], we reasoned that targeting Cdk2 may be an attractive alternative given the current availability of small molecule Cdk2 inhibitors.

The objective of this study was to investigate the potential of Cdk2 inhibitor to suppress ovary tumor progression. With a panel of established ovarian cancer cell lines, we found that majority of ovarian cancer cell lines with CCNE1 overexpression possessed *CCNE1* gene amplification. Immunohistochemistry study with primary ovary tumor specimens showed that over 40% of ovary tumor specimens were positive for CCNE1 staining; in contrast, CCNE1 staining was either negative or very low in normal ovary and benign ovary tumor specimens. However, the status of elevated CCNE1 expression was not relevant to the properties of cell growth and metastatic colonization in ovarian cancer cell lines while CCNE1 staining was not associated with pathological grades of all three histological types of ovarian cancer (serous, mucinous and endometrioid). Despite lack of clear association between CCNE1 expression and tumorigenic behaviors, CCNE1 is critical for the growth of ovarian cancer cell lines with elevated CCNE1 expression

because knockdown of CCNE1 diminished the growth of cells with CCNE1 overexpression but not cells without CCNE1 overexpression. To determine the effect of Cdk2 inhibitor on ovarian cancer cell growth, we showed that ovarian cancer cells with elevated CCNE1 expression are at least 40 times more sensitive to Cdk2 inhibitor SNS-032 than those without CCNE1 overexpression, immortalized OECs and FTSECs. Finally, we demonstrated that SNS-032 effectively suppressed the tumorigenicity of ovarian cancer cells with elevated CCNE1 expression by prolonging the survival of animals bearing tumors derived from ovarian cancer cells with elevated CCNE1 expression and inhibiting peritoneal metastatic colonization.

RESULTS

CCNE1 expression in established ovarian cancer cell lines

Elevation of CCNE1 level has been reported in various histological types of human ovarian tumors including HGSOC [5, 7]. Integrated analysis of ovarian carcinoma from the study of TCGA further showed that *CCNE1* gene is amplified in 15-20% of HGSOC [4]. To determine if elevated CCNE1 expression is linked to *CCNE1* gene amplification in ovarian cancer, we initially examined the level of CCNE1 mRNA and protein in a panel of established ovarian cancer cell lines, immortalized ovary epithelial cells (OECs) and FTSECs. The abundance of CCNE1 mRNA and protein were generally correlated in all cell lines examined (Figure 1A and 1B). Level of CCNE1 was elevated in OVCAR3, OVCAR5, OVCAR8 and OCC1 cells compared to that in OECs or FTSECs whereas the remaining cell lines displayed either similar or lower level of CCNE1 compared to OECs and FTSECs (Figure 1A and 1B). We subsequently isolated genomic DNA and performed qPCR to analyze the copy number of *CCNE1* gene in these cell lines. Comparing to that in OECs or FTSECs, *CCNE1* gene was not amplified in ovarian cancer cell lines without CCNE1 overexpression (Figure 1C). Among lines with elevated CCNE1 expression, *CCNE1* gene amplification was detected in OVCAR3, OVCAR5 and OVCAR8 cell lines (Figure 1C). However, relative copy number of *CCNE1* gene in OCC1 cells was the same as that in OECs and FTSECs (Figure 1C). Our data show that *CCNE1* gene amplification is present in majority of ovarian cancer cell lines with elevated CCNE1 overexpression, thus indicating that *CCNE1* gene amplification is at least one of the principal factors contributing to CCNE1 overexpression in ovarian cancer.

To investigate whether the status of elevated CCNE1 expression could be linked to tumorigenic behaviors of ovarian cancer cell lines, we first assessed cell growth

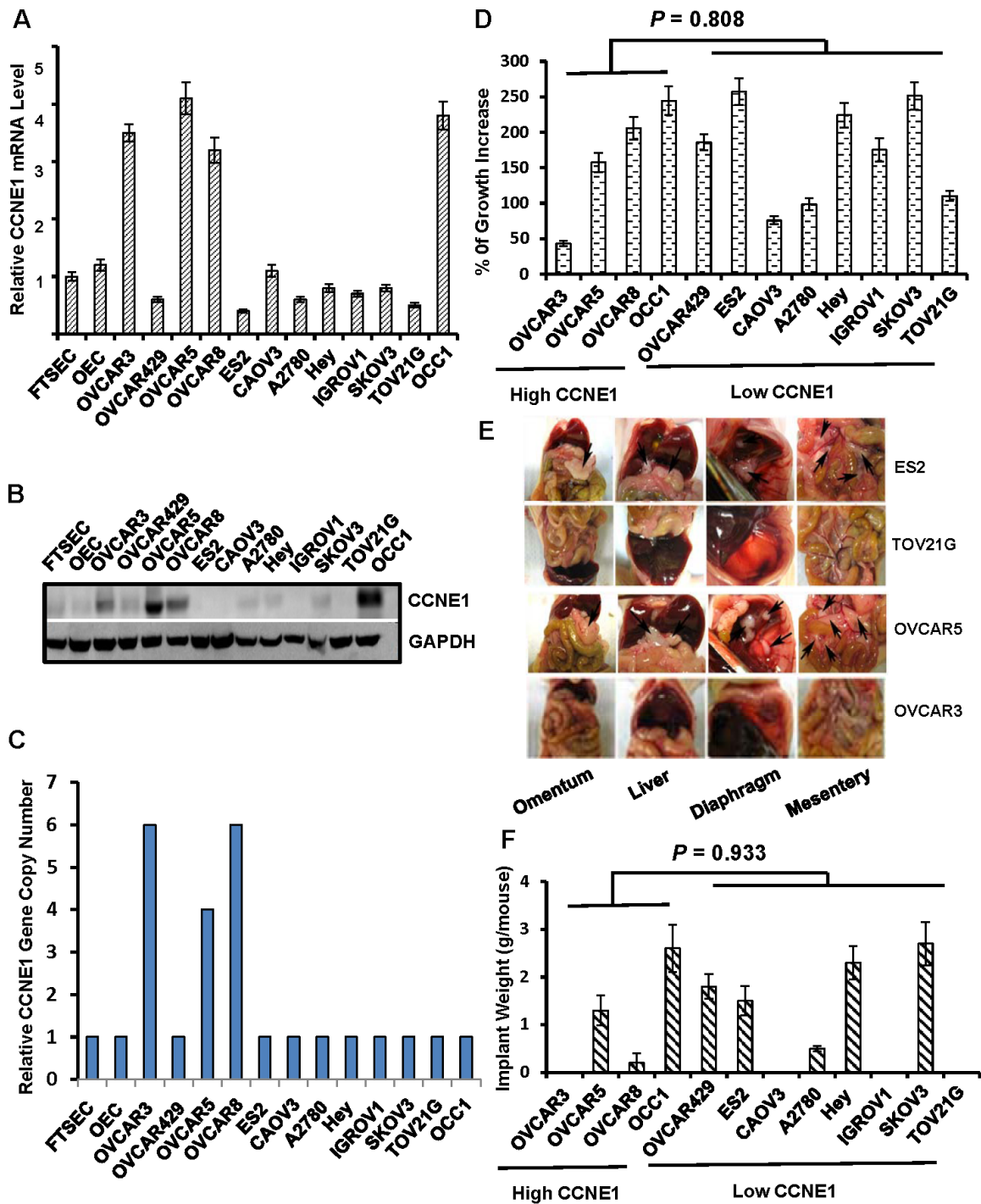


Figure 1: The status of CCNE1 overexpression is not associated with tumorigenic behaviors in established ovarian cancer cells. **A.** Total RNA was isolated from overnight-cultured cells and subjected to qRT-PCR to quantitate the amount of CCNE1 mRNA. β -actin mRNA was used as an internal standard for normalization. **B.** Overnight-cultured cells were harvested and cell lysates were subjected to immunoblotting to detect CCNE1 protein using CCNE1 mAb. Membrane was stripped and reprobed with GAPDH polyclonal antibody for loading normalization. **C.** Genomic DNA was isolated from overnight-cultured cells and subjected to qPCR to analyze copy number of *CCNE1* gene. *ACTB* gene was used for normalization. **D.** Cells (50,000/well) were plated in 24-well plates for overnight and then cultured for 2 days followed by MTT assay. % of growth increase was calculated as $[(OD_{\text{overnight}} - OD_{\text{end}}) / OD_{\text{overnight}}] \times 100$. **E.** Cells (1×10^7 cell/mouse) from various ovarian cancer lines were intraperitoneally injected to nude mice for 4 weeks to allow metastatic colonization. Images are the views of various areas in peritoneal cavity. Arrows point to metastatic implants. **F.** Metastatic implants were collected and weighed. Data are means \pm SE. $n = 6$.

of these cell lines. MTT assay showed an increase of 43% to 257% in 2-day growth period among these lines (Figure 1D). However, we were unable to detect an apparent association between the abundance of CCNE1 and growth rate among them ($P = 0.808$ between with and without CCNE1 overexpression). Subsequent peritoneal metastatic colonization revealed that some high CCNE1 expressers were capable of undergoing efficient metastatic colonization while others were not (Figure 1E and 1F). Similarly, ovarian cancer cell lines without CCNE1 overexpression could also be either metastatic or non-metastatic (Figure 1E and 1F; $P = 0.933$ between with and without CCNE1 overexpression). These data thus failed to establish a correlation between the status of CCNE1 overexpression and tumorigenic potential in ovarian cancer cell lines.

CCNE1 expression in human ovarian tumors

Previous studies reveal that *CCNE1* gene amplification correlates with tumor progression and predicts a poor prognosis in ovarian cancer patients [7, 9, 17]. However, our *in vitro* studies with established ovarian cancer cell lines failed to establish a correlation between CCNE1 expression and tumorigenic potential (Figure 1D, 1E and 1F). To understand this differentiation, we examined CCNE1 staining in human ovarian tumor

specimens by performing immunohistochemistry on a tissue array that contained normal, benign and ovarian tumor tissues. CCNE1 staining was negative or low in all normal ovary and benign tumor tissues (Table 1, Figures 2A, S1A, 2B and S1B). The only clear cell type ovary tumor specimen showed low CCNE1 staining (Table 1 and Figure 2C). In contrast, 43.8% of serous (21/48), 55.6% of mucinous (10/18) and 40.0% of endometrioid ovary tumor specimens (12/30) were strong for CCNE1 staining (Table 1, Figures 2D, S1C, 2E, S1D, 2F and S1E). The staining of CCNE1 was not associated with histological types or correlated with pathological grades of the disease (Table 1). These results were consistent with the data generated from ovarian cancer cell lines, in which CCNE1 level is found not to be correlated with the tumorigenic potential of ovarian cancer cell lines (Figure 1).

Presence of CCNE1 is critical for growth of ovarian cancer cells with elevated CCNE1 expression

Although we were unable to detect clear correlation between CCNE1 and tumorigenic potential of ovarian cancer cells (Figure 1), the observation of elevated CCNE1 expression in over 40% ovary tumor specimens (Table 1 and Figure 2) raised the possibility that the presence of

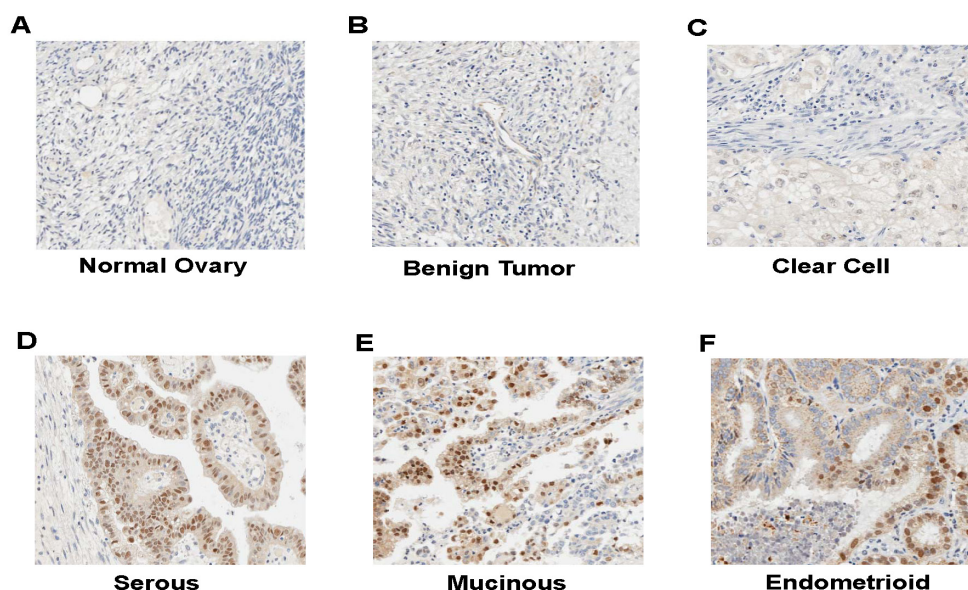


Figure 2: Immunohistochemistry of CCNE1 on ovary tumor specimens. A. Normal ovary tissue. B. Benign ovary tumor tissue. C. Clear cell type of ovary tumor specimen. D. Serous type of ovary tumor specimen. E. Mucinous type of ovary tumor specimen. F. Endometrioid type of ovary tumor specimen.

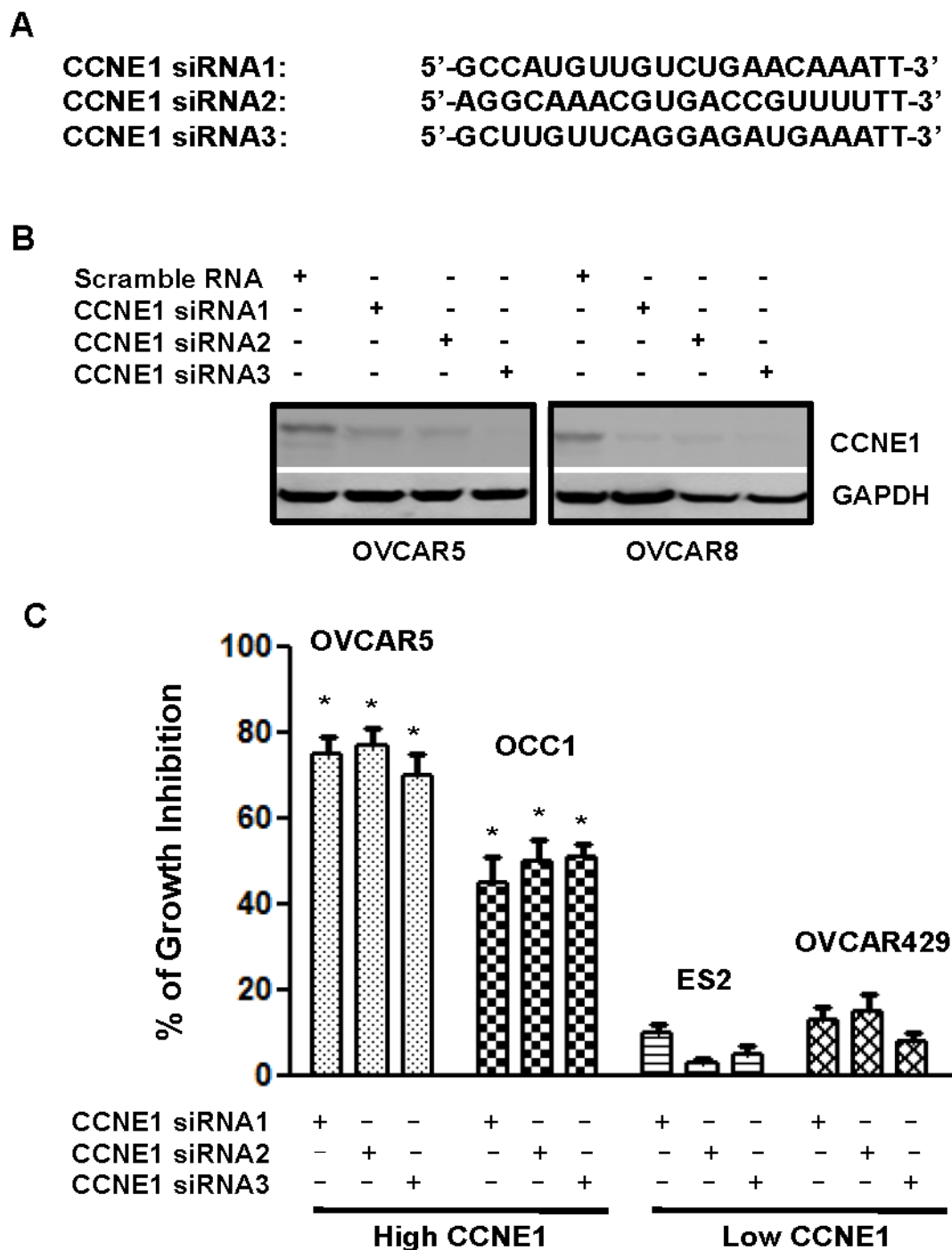


Figure 3: Ovarian cancer cells with elevated CCNE1 expression is sensitive to CCNE1 knockdown. A. Sequences of CCNE1 siRNAs. B. OVCAR5 and OVCAR8 cells were transfected with scrambled control or CCNE1 siRNAs for 3 days, then lysed and lysates were subjected to immunoblotting to detect CCNE1 with CCNE1 mAb. Membrane was stripped and reprobed with GAPDH polyclonal antibody for loading normalization. C. Cells (50,000 cells/well of 24-well plate) were transfected with scrambled control or CCNE1 siRNAs for overnight, then re-fed with fresh medium and cultured for 4 days prior to MTT assay to assess cell growth. % of growth inhibition = $[(OD_{control} - OD_{siRNA}) / OD_{control}] \times 100$. Data are means \pm SE. $n = 4$. *, $P < 0.005$ vs scrambled control.

Table 1: Correlation between the status of CCNE1 staining and clinicopathological parameters of ovarian cancer patients

	Total No. of patients	CCNE1 Staining		P value
		Negative or Low (%)	Positive (%)	
Histological types				0.565
Serous	48	27 (56.3%)	21 (43.7%)	
Mucinous	18	8 (44.4%)	10 (55.6%)	
Endometrioid	30	18 (40.0%)	12 (60.0%)	
Pathologic Grade				0.582
I	30	15 (50.0%)	15 (50.0%)	
II	27	14 (51.9%)	13 (48.1%)	
III	39	24 (47.4%)	15 (52.6%)	

CCNE1 may be only involved in the tumorigenicity of ovarian cancer cells with elevated CCNE1 expression. To test this possibility, we designed three siRNAs that target various regions of CCNE1 mRNA (Figure 3A). Immunoblotting to detect CCNE1 showed that all three CCNE1 siRNAs effectively diminished the level of CCNE1 in OVCAR5 and OVCAR8 cells when compared with the scrambled control (Figure 3B). With these siRNAs, MTT assay showed that knockdown of CCNE1 led to 65-90% of reduction in cell growth in cell lines with elevated CCNE1 expression (OVCAR3, OVCAR5, OVCAR8 and OCC1) (Figures 3C and S2). However, CCNE1 siRNAs did not significantly alter the growth of ovarian cancer cell lines without CCNE1 overexpression (ES2, OVCAR429, IGROV1, SK-OV3) (Figure 3C and S2). Since *CCNE1* gene is not amplified in OCC1 cells (Figure 1C), these results suggest that the presence of CCNE1 is critically important for the growth of ovarian cancer cells with elevated CCNE1 expression regardless of *CCNE1* gene amplification status.

Ovarian cancer cells with elevated CCNE1 expression are greatly more sensitive to Cdk2 inhibitor

CCNE1 forms a complex with and functions as a regulatory subunit of Cdk2 to regulate cell cycle G1/S transition [11]. We initially performed immunoblotting to detect Cdk1 and Cdk2 in ovarian cancer cell lines. Levels of Cdk1 and Cdk2 varied in these cell lines (Figure 4A). However, we failed to detect a correlation between the abundance of CCNE1 and Cdk1 or Cdk2. Recent study showed that ovarian cancer cells overexpressing CCNE1 exhibited greater Cdk2 activity [12]. We thus hypothesized that ovarian cancer cells with elevated CCNE1 expression would be more sensitive to the suppression of Cdk2 activity. To test this hypothesis, cell lines with and without elevated CCNE1 expression were

treated with varying concentration of selective inhibitor to Cdk1 JNJ-7706621 [18] or Cdk2 SNS-032 [19]. MTT assay showed that OVCAR429 was the most sensitive line to JNJ-7706621 among ovarian cancer cell lines without CCNE1 overexpression which had an IC₅₀ of 0.55 μM while OVCAR5 was the least sensitive line among ovarian cancer cell lines with elevated CCNE1 expression which had an IC₅₀ of 2.02 μM (Figure 4B). This reveals a less than 4-fold difference in the sensitivity to JNJ-7706621 between cell lines with and without CCNE1 overexpression ($P = 0.037$ between with and without CCNE1 overexpression). In contrast, IC₅₀ of SNS-032 in ES2, the most sensitive ovarian cancer cell line among those without CCNE1 overexpression was 20.05 μM while IC₅₀ of SNS-032 in OVCAR3, the least sensitive one among those with elevated CCNE1 expression was 0.53 μM (Figure 4C). This uncovers a 40-fold difference in the sensitivity to Cdk2 inhibitor between ovarian cancer cell lines with and without CCNE1 overexpression ($P = 0.003$). In a parallel experiment, we further analyzed the sensitivity of immortalized OECs and FTSECs to SNS-032. IC₅₀s of OECs and FTSECs in a 4-day treatment period were 25.21 and 31.44 μM respectively (Figure 4C), resembling to those observed in ovarian cancer cells without CCNE1 overexpression.

To determine whether SNS-032-led cell growth suppression was the consequence of cell apoptosis, OCC1 and OVCAR429 cells were treated with 0.5 or 2 μM of SNS-032 for 2 days followed by Annexin V staining-based flow cytometry to detect apoptotic cells (Figure 4D and 4E). Treatment of SNS-032 resulted in a significant increase in the percentage of apoptotic cells in OCC1, a line with elevated CCNE1 expression (Figure 4D). In contrast, identical concentration of SNS-032 only marginally increased the percentage of apoptotic cells in OVCAR429, a line without CCNE1 overexpression (Figure 4E). These results demonstrate that Cdk2 inhibitor SNS-032 selectively induces apoptosis in ovarian cancer cells with elevated CCNE1 expression.

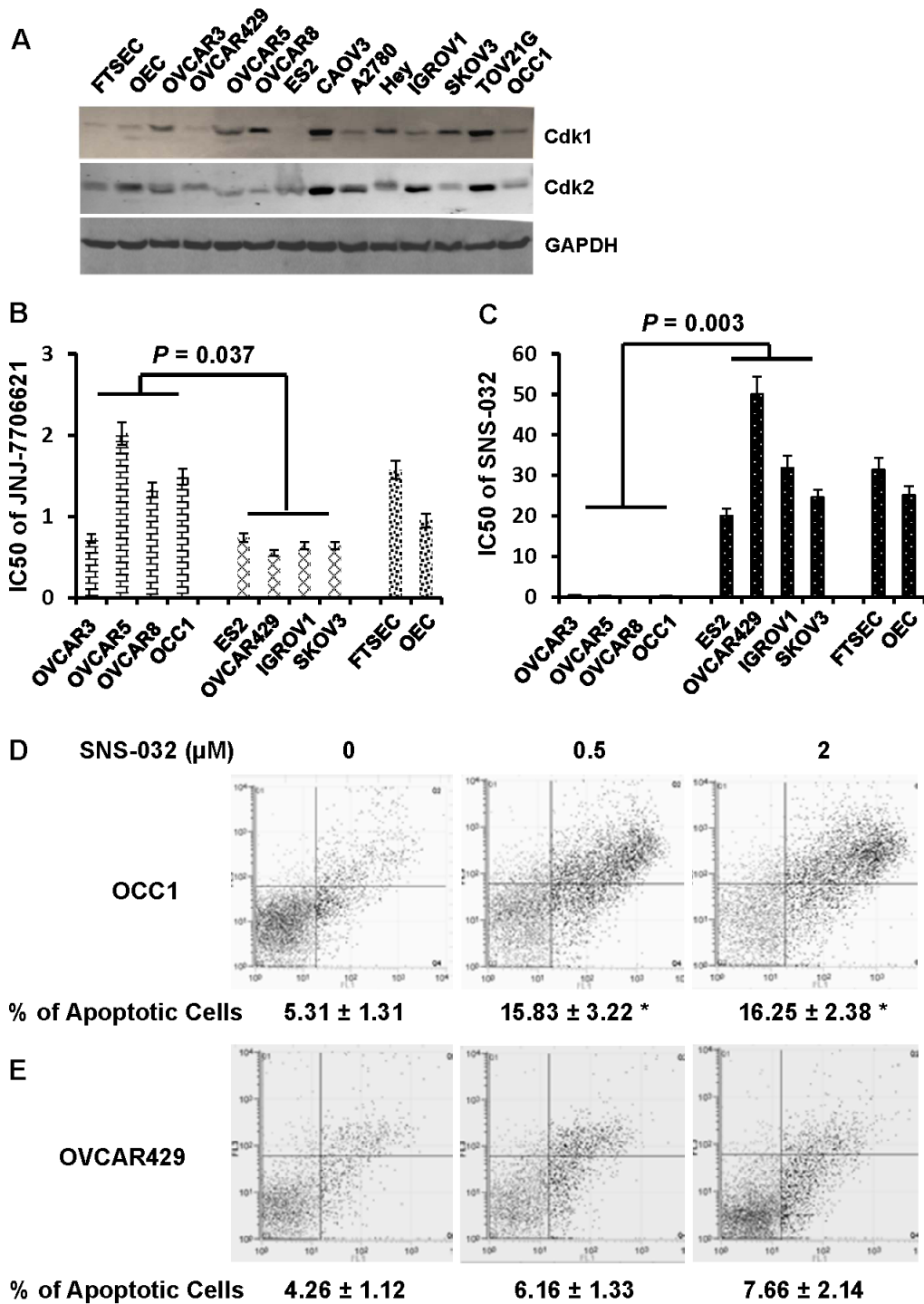


Figure 4: Cdk2 inhibitor SNS-032, but not Cdk1 inhibitor JNJ-7706621 selectively inhibits growth of ovarian cancer cells with elevated CCNE1 expression by inducing apoptosis. **A.** Overnight-cultured cells were harvested and cell lysates were subjected to immunoblotting to detect Cdk1 and Cdk2 protein using the respective antibodies. Membrane was stripped and reprobed with GAPDH polyclonal antibody for loading normalization. **B, C.** Ovarian cancer cells (40,000 cells/well) were plated in 24-well plates for overnight and varying concentrations of JNJ-7706621 **B.** or SNS-032 **C.** were added to cells for 4 days. Cell growth was evaluated by MTT assay and IC50 was estimated as the concentration required for reach 50% growth reduction comparing to untreated cells. **D, E.** OCC1 **D.** or OVCAR429 cells **E.** were treated with 0.5 or 2 μM SNS-032 for 2 days, then stained with Annexin V-FITC/propidium iodide and analyzed by FACS. Data are means \pm SE. $n = 4$. *, $P < 0.005$ vs 0 μM of SNS-032.

Cdk2 inhibitor prolongs the survival of mice bearing tumors derived from cells with elevated CCNE1 expression

The observation that Cdk2 inhibitor SNS-032 selectively induces apoptosis in ovarian cancer cells with elevated CCNE1 expression prompted us to investigate its efficacy to suppress ovarian tumor progression with the well-established ovarian tumor peritoneal metastatic colonization model [20, 21]. Female athymic nude mice

were intraperitoneally injected with OCC1, OVCAR429, ES2 or OVCAR5 cells and then received SNS-032 twice a week starting 5 days after tumor cell injection. Mice receiving any of these cell lines died between 4 to 6 weeks (Figures 5A, 5B, S3A and S3B). Administering SNS-032 slightly increased the lifespan of mice receiving OVCAR429 cells while exhibited no improvement on mice injected with ES2 cells (Figure 5B and S3B). In contrast, SNS-032 greatly prolonged the survival of mice injected with OCC1 and OVCAR5 cells (Figure 5A and S3A). In fact, 30% of OCC1 cell-injected mice treated

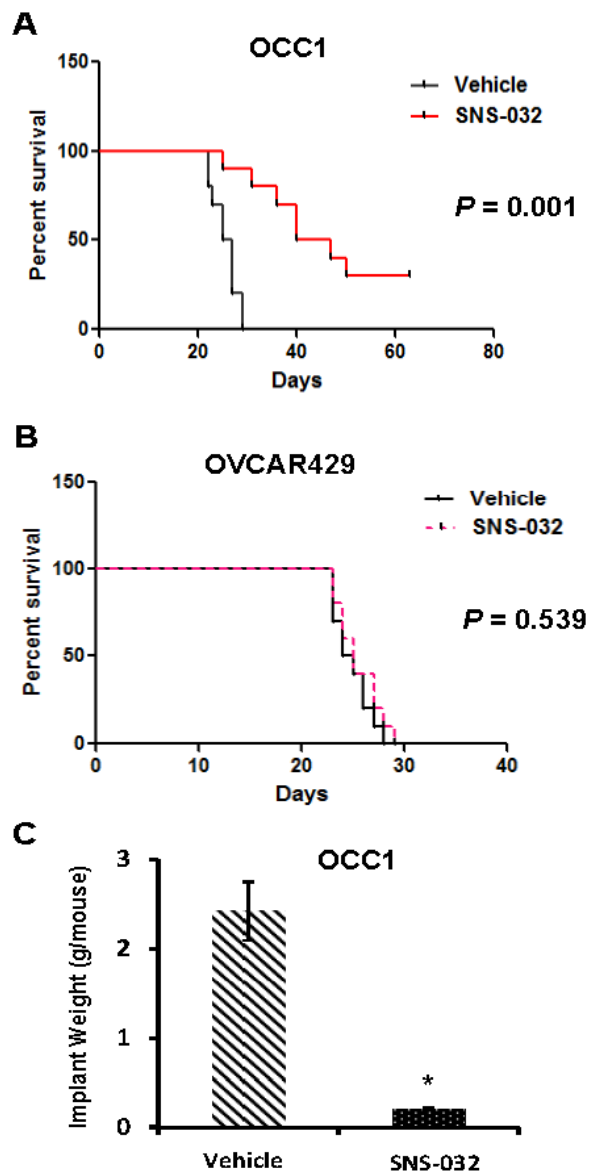


Figure 5: SNS-032 suppresses tumorigenicity of ovarian cancer cells with CCNE1 overexpression. A., B. Kaplan-Meier curve summarizing survival of mice injected with OCC1 A. and OVCAR429 cells B. Female athymic nude mice were injected *i.p.* with OCC1 or OVCAR429 cells (1×10^7 cells/mouse) for 5 days followed by administration of 30 mg/kg SNS-032 twice per week until animal died. C. OCC1 cells (1×10^7 cells/mouse) were injected *i.p.* to nude mice for 5 days followed by SNS-032 treatment for 3 weeks. Mice were sacrificed and metastatic implants were collected/weighed. Data are means \pm SE. $n = 10$. *, $P < 0.001$ vs vehicle.

with SNS-032 survived longer than 9 weeks while all OCC1 cell-injected mice receiving vehicle died within 4 weeks (Figure 5A). These results show that SNS-032 promotes the survival of mice bearing tumors derived from ovarian cancer cells with elevated CCNE1 expression but not mice bearing tumors derived from cells without CCNE1 overexpression.

In a parallel set of experiment, we determined the effect of SNS-032 on metastatic colonization. Mice were injected with OCC1 cells for 5 days, and then administered with vehicle or SNS-032 for 3 weeks followed by collection metastatic implants from sacrificed animals. Measurement of implant weight showed that mice receiving SNS-032 displayed an average of 85% less metastatic implants than control mice (administered with vehicle) (Figure 5C). These results suggest that prolonged survival of tumor-bearing mice is most likely the consequence of suppressed metastatic colonization.

DISCUSSION

CCNE1 is abnormally expressed in various tumor types [11, 22]. Its role in tumorigenesis has been well established in various tumor models [15, 23]. In ovarian cancer, *CCNE1* gene was amplified in approximately 20% of ovary tumor specimens including both serous and endometrioid types [2, 4, 5]. Immunohistochemistry studies further indicate that CCNE1 overexpression may contribute the malignancies of ovary tumors [7, 9]. Here, we show that elevated CCNE1 expression is detected in more than 30% of the established ovarian cancer cell lines (Figure 1A and 1B) and majority of the lines with CCNE1 overexpression displayed *CCNE1* gene amplification (Figure 1C). Our results support the notion that *CCNE1* gene amplification is at least one of the key factors contributing to elevated CCNE1 expression in ovarian cancer.

Consistent with published immunohistochemistry studies [7, 9, 24], we showed that over 40% of primary ovary tumor specimens were positive for CCNE1 staining (Table 1 and Figure 2). Although CCNE1 staining was negative or low in all normal ovary tissues or benign ovary tumor specimens, we did not detect a correlation between CCNE1 staining and pathological grades in ovary tumor specimens (Table 1). This result concurs with the observation that the status of CCNE1 overexpression was not associated with growth rate and metastatic potential among the established ovarian cancer cell lines (Figure 1). An early study reported that high CCNE1 expression is a significant and independent predictor for prolonged overall survival in late stage ovarian cancer patients [10]. Although data from our studies do not support CCNE1 as a key factor to promote tumorigenic behaviors including cell growth and metastatic potential in ovarian cancer cells, it does not rule out the potential of CCNE1 as a potent tumor-promoting factor in ovarian cancer

cells with elevated CCNE1 expression. In fact, forced CCNE1 expression accelerates cell growth and increases chemosensitivity in ovarian cancer cells [6, 13]. We also showed that knockdown of CCNE1 led to the suppression of cell growth of ovarian cancer cells with inherently elevated CCNE1 expression (Figure 3).

Although we failed to detect a clear correlation between CCNE1 level and malignancies in both established ovarian cancer cell lines as well as primary tumor specimens (Figures 1 and 2), the frequent CCNE1 gene amplification in ovarian cancer and the ability of CCNE1 to facilitate the formation of HGSOE from FTSECs indicates that ovarian cancer cells with elevated CCNE1 expression could have developed addiction to CCNE1 overexpression for cell growth/survival. This possibility is clearly supported by our observation that the growth of ovarian cancer cell lines with CCNE1 overexpression are greatly inhibited by CCNE1 knockdown while CCNE1 siRNAs did not significantly alter the growth of lines without CCNE1 overexpression (Figure 3). Our results are also in agreement with two recent studies reporting that depleting CCNE1 leads to the suppression of ovarian cancer cell proliferation [6, 16]. Oncogene addiction is dependence on oncogene even though this oncogene is not needed before its activation [25, 26]. Some of the well-established examples on oncogene addiction include amplification of HER2 in breast cancer [27], mutated EGFR in non-small cell lung cancer [28], mutated BRAF in melanomas [29] and Bcr-Abl in chronic myeloid leukemia [30, 31]. Our finding that some ovarian cancer cells are addicted to the presence of CCNE1 indicates that CCNE1 may be a driver oncogene to initiate ovarian cancer.

Interfering with CCNE1 function may be an effective strategy to suppress CCNE1-overexpressing ovary tumors, the nature of CCNE1 as a regulatory subunit of CDK complex rather than as an enzyme or receptor indicates that CCNE1 itself is not likely to be an ideal drug target. Because CCNE1 facilitates cell cycle transition mainly by forming complex with Cdk2 (CCNE1 may also complex with Cdk1 and Cdk4 to a lesser extent) [11], we speculated that blocking CCNE1 function may be achieved by targeting the Cdks that interact with CCNE1. In this study, we show that ovarian cancer cell lines with elevated CCNE1 expression are at least 40 times more sensitive to Cdk2 inhibitor SNS-032 than lines without inherent CCNE1 overexpression, non-cancerous OECs and FTSECs (Figure 4). SNS-032 apparently inhibits cell growth of inherently CCNE1-overexpressing ovarian cancer cells by inducing apoptosis (Figure 4). Since Cdk1 inhibitor JNJ-7706621 was not as selective as SNS-032 in suppressing cell growth between ovarian cancer cell lines with and without elevated CCNE1 expression (Figure 4), our results raise the possibility that a subset of ovarian cancer patients with elevated CCNE1 level may be helped by Cdk2 inhibitors. This possibility is supported by our

observation that Cdk2 inhibitor SNS-032 suppressed metastatic colonization of CCNE1-overexpressing ovarian cancer cells and greatly prolonged the survival of mice bearing ovary tumors with CCNE1 overexpression (Figure 5). In conclusion, our study has laid a foundation on using currently available Cdk2 inhibitor for ovary tumors that exhibit elevated CCNE1 expression.

MATERIALS AND METHODS

Cells, siRNAs and other reagents

Immortalized human ovarian epithelial cells and immortalized human fallopian tube secretory epithelial cells were purchased from ABM (Richmond, BC, Canada) and maintained according to manufacturer's protocol. All human ovarian cell lines were maintained in DMEM containing 10% FCS at 37°C in a humidified incubator supplied with 5% CO₂. All siRNAs were purchased from Shanghai GenePharma (Shanghai, China). Cdk1 inhibitor JNJ-7706621 and Cdk2 inhibitor SNS-032 (BMS-387032) were purchased from Selleckchem (Houston, TX). Information for primer sequences is included in Supplementary Data.

qRT-PCR and qPCR

Total RNA was extracted from cells using Trizol (Life Technologies, Carlsbad, CA), treated by DNaseI and reverse transcribed with SuperScriptase II (Life Technologies). Generated cDNA was subjected to quantitative PCR to measure CCNE1 and β -actin mRNA levels with specific primer sets. The expression levels were standardized by comparing the Ct values of target to that of β -actin mRNA. To measure copies of *CCNE1* gene in cells, genomic DNA was isolated using DNAzol (Life Technologies) and used as template for qPCR. The copy number of *CCNE1* gene was standardized to β -actin gene.

Immunoblotting

To determine the amount of CCNE1, Cdk1 or Cdk2 in cells, overnight-cultured cells were harvested using radio-immunoprecipitation assay (RIPA) buffer. To determine the effect of CCNE1 siRNAs on CCNE1 expression, cells were transfected with scrambled control or CCNE1 siRNAs for 3 days and then harvested using RIPA. Cellular proteins were resolved by 12% SDS-PAGE, transferred to nitrocellulose membrane and blocked before probing with anti-CCNE1 mAb (Cell Signaling Technology, Danvers, MA), anti-Cdk2 mAb (Life Technologies), Cdk2 mAb (Cell Signaling Technology) or anti-GAPDH polyclonal antibody (Santa

Cruz Biotechnology, Santa Cruz, CA).

Histochemistry

CCNE1 level in ovary tumors and normal ovary tissues were evaluated by IHC using anti-CCNE1 mAb on commercial tissue arrays (Super Biotek, Shanghai, China) as previously described [32, 33]. The array contained 10 normal ovary tissues, 10 benign ovarian tumor specimens and 97 ovarian tumor samples (1 clear cell, 48 serous, 18 mucinous and 30 endometrioid). Extent of immunostaining was given a modified histochemical score (MH-score) that considers both the intensity and the percentage of cells stained at each intensity. Samples with below the average MH-score were considered as no/weak staining while samples with above the average MH-score considered as strong staining.

MTT assay

Cell growth was assayed by MTT as described previously [34]. Briefly, 5x10⁴ cells were seeded into 24-well culture plates and allowed to grow for 2-4 days prior to the addition of MTT. Dilutions of pharmacologic agents in growth media were done in four replicate rows per cell type and per dilution. Plates were then incubated in a humidified incubator in 5% CO₂ at 37°C. At the time points indicated, 100 μ L of MTT solution (5 mg/mL MTT in PBS) were added to a total volume of 1 ml and incubated in 5% CO₂ at 37°C for 4 h. Formazan crystals were dissolved with 0.5 ml DMSO and absorbance at 570 nm was determined with a plate reader. To determine the effect of CCNE1-knockdown on cell growth, cells were transfected with CCNE1 or control siRNAs for 4 days prior to MTT assay. Growth inhibition was calculated with the formula of [(absorbance of treated – absorbance of control)/(absorbance of control)] x 100%.

Apoptosis detection

Apoptosis was quantified using an Annexin V-FITC detection kit (BD Biosciences, San Jose, CA) according to manufacturers' instructions. Briefly, cells were treated with 0.5 or 2 μ M Cdk2 inhibitor for 2 days, then trypsinized and resuspended in binding buffer (100 mM HEPES, 1.4 M NaCl, 25 mM CaCl₂, pH 7.4) containing Annexin V-FITC and propidium iodide. Stained cells were analyzed by fluorescence activating cell sorter (FACS) (Becton Dickinson, CA, USA) and the percentage of apoptotic cell population was determined using ModFit LT 3.0 software (Becton Dickinson, CA, USA).

Peritoneal metastatic olonization assay

Peritoneal metastatic colonization assays were performed as previously described [20]. Female athymic nude mice (BALB/c, 6 weeks of age) were obtained from Shanghai Laboratory Animal Research Center (Shanghai, China). To determine metastatic potential of each ovarian cancer cell line, cells grown in log-phase were resuspended in PBS and intraperitoneally injected into nude mice at 10^7 cells/mouse. Three weeks after injection, the mice were sacrificed and autopsied. Visible metastatic implants were collected and weighed. To determine the effect of SNS-032 in peritoneal metastatic colonization, nude mice were injected with ES2, OCC1, OVCAR429 and OVCAR5 cells (10^7 cells/mouse), and SNS-032 dissolved in 5% Propylene glycol was administered by intraperitoneal injection twice per week at 30 mg/kg 5 days post-operation. A subset of mice receiving OCC1 cells were euthanized 3 weeks post SNS-032 treatment and autopsied. Visible metastatic implants were collected and weighed. Animal housing and experimental conditions were in compliance with the protocol approved by the Institutional Animal Care and Use Committee at the Shanghai University of Traditional Chinese Medicine.

Statistical analysis

Statistical analyses of cell growth, metastatic implant weights and CCNE1 mRNA levels were performed by ANOVA and student *t* test. Chi-square test was used to compare covariates between CCNE1 staining and clinicopathological parameters. Mann-Whitney test was used to analyze the significance in mouse survival. Statistical analyses were aided by SPSS (release 15.0; SPSS Inc). $P < 0.05$ was considered to be significant.

ACKNOWLEDGMENTS

This study was supported by grants from E-Institutes of Shanghai Municipal Education Commission (Project E03008), “085” First-Class Discipline Construction Innovation Science and Technology Support Project of Shanghai University of TCM (085ZY1206) and DoD OC120313 (W81XWH-13-1-0122).

CONFLICTS OF INTEREST

The authors declare that they have no conflict of interest.

REFERENCES

- Jayson GC, Kohn EC, Kitchener HC and Ledermann JA. Ovarian cancer. *Lancet*. 2014; 384:1376-1388.
- Nakayama K, Nakayama N, Jinawath N, Salani R, Kurman RJ, Shih Ie M and Wang TL. Amplicon profiles in ovarian serous carcinomas. *Int J Cancer*. 2007; 120:2613-2617.
- Lambros MB, Fiegler H, Jones A, Gorman P, Roylance RR, Carter NP and Tomlinson IP. Analysis of ovarian cancer cell lines using array-based comparative genomic hybridization. *The Journal of pathology*. 2005; 205:29-40.
- Integrated genomic analyses of ovarian carcinoma. *Nature*. 2011; 474:609-615.
- Marone M, Scambia G, Giannitelli C, Ferrandina G, Masciullo V, Bellacosa A, Benedetti-Panici P and Mancuso S. Analysis of cyclin E and CDK2 in ovarian cancer: gene amplification and RNA overexpression. *Int J Cancer*. 1998; 75:34-39.
- Nakayama N, Nakayama K, Shamima Y, Ishikawa M, Katagiri A, Iida K and Miyazaki K. Gene amplification CCNE1 is related to poor survival and potential therapeutic target in ovarian cancer. *Cancer*. 2010; 116:2621-2634.
- Rosen DG, Yang G, Deavers MT, Malpica A, Kavanagh JJ, Mills GB and Liu J. Cyclin E expression is correlated with tumor progression and predicts a poor prognosis in patients with ovarian carcinoma. *Cancer*. 2006; 106:1925-1932.
- Lv H, Shi Y, Zhang L, Zhang D, Liu G, Yang Z, Li Y, Fei F and Zhang S. Polyploid giant cancer cells with budding and the expression of cyclin E, S-phase kinase-associated protein 2, stathmin associated with the grading and metastasis in serous ovarian tumor. *BMC cancer*. 2014; 14:576.
- Sui L, Dong Y, Ohno M, Sugimoto K, Tai Y, Hando T and Tokuda M. Implication of malignancy and prognosis of p27(kip1), Cyclin E, and Cdk2 expression in epithelial ovarian tumors. *Gynecologic oncology*. 2001; 83:56-63.
- Pils D, Bachmayr-Heyda A, Auer K, Svoboda M, Auner V, Hager G, Obermayr E, Reiner A, Reinthaller A, Speiser P, Braicu I, Sehouli J, Lambrechts S, Vergote I, Mahner S, Berger A, et al. Cyclin E1 (CCNE1) as independent positive prognostic factor in advanced stage serous ovarian cancer patients - a study of the OVCAD consortium. *European journal of cancer*. 2014; 50:99-110.
- Siu KT, Rosner MR and Minella AC. An integrated view of cyclin E function and regulation. *Cell Cycle*. 2012; 11:57-64.
- Bedrosian I, Lu KH, Verschraegen C and Keyomarsi K. Cyclin E deregulation alters the biologic properties of ovarian cancer cells. *Oncogene*. 2004; 23:2648-2657.
- Etemadmoghadam D, George J, Cowin PA, Cullinane C, Kansara M, Gorringer KL, Smyth GK and Bowtell DD. Amplicon-dependent CCNE1 expression is critical for clonogenic survival after cisplatin treatment and is correlated with 20q11 gain in ovarian cancer. *PLoS ONE*. 2010; 5:e15498.
- Etemadmoghadam D, deFazio A, Beroukhir R, Mermel C, George J, Getz G, Tothill R, Okamoto A, Raeder MB, Harnett P, Lade S, Akslen LA, Tinker AV, Locandro B,

- Alsop K, Chiew YE, et al. Integrated genome-wide DNA copy number and expression analysis identifies distinct mechanisms of primary chemoresistance in ovarian carcinomas. *Clin Cancer Res.* 2009; 15:1417-1427.
15. Karst AM, Jones PM, Vena N, Ligon AH, Liu JF, Hirsch MS, Etemadmoghadam D, Bowtell DD and Drapkin R. Cyclin E1 deregulation occurs early in secretory cell transformation to promote formation of fallopian tube-derived high-grade serous ovarian cancers. *Cancer Res.* 2014; 74:1141-1152.
 16. Etemadmoghadam D, Au-Yeung G, Wall M, Mitchell C, Kansara M, Loehrer E, Batzios C, George J, Ftouni S, Weir BA, Carter S, Gresshoff I, Mileskin L, Rischin D, Hahn WC, Waring PM, et al. Resistance to CDK2 inhibitors is associated with selection of polyploid cells in CCNE1-amplified ovarian cancer. *Clinical cancer research : an official journal of the American Association for Cancer Research.* 2013; 19:5960-5971.
 17. Mayr D, Kanitz V, Anderegg B, Luthardt B, Engel J, Lohrs U, Amann G and Diebold J. Analysis of gene amplification and prognostic markers in ovarian cancer using comparative genomic hybridization for microarrays and immunohistochemical analysis for tissue microarrays. *Am J Clin Pathol.* 2006; 126:101-109.
 18. Emanuel S, Rugg CA, Gruninger RH, Lin R, Fuentes-Pesquera A, Connolly PJ, Wetter SK, Hollister B, Kruger WW, Napier C, Jolliffe L and Middleton SA. The *in vitro* and *in vivo* effects of JNJ-7706621: a dual inhibitor of cyclin-dependent kinases and aurora kinases. *Cancer Res.* 2005; 65:9038-9046.
 19. Chen R, Wierda WG, Chubb S, Hawtin RE, Fox JA, Keating MJ, Gandhi V and Plunkett W. Mechanism of action of SNS-032, a novel cyclin-dependent kinase inhibitor, in chronic lymphocytic leukemia. *Blood.* 2009; 113:4637-4645.
 20. Chen H, Wu X, Pan ZK and Huang S. Integrity of SOS1/EPS8/ABI1 tri-complex determines ovarian cancer metastasis. *Cancer Res.* 2010; 70:9979-9990.
 21. Yamada SD, Hickson JA, Hrobowski Y, Vander Griend DJ, Benson D, Montag A, Karrison T, Huo D, Rutgers J, Adams S and Rinker-Schaeffer CW. Mitogen-activated protein kinase kinase 4 (MKK4) acts as a metastasis suppressor gene in human ovarian carcinoma. *Cancer Res.* 2002; 62:6717-6723.
 22. Malumbres M and Barbacid M. Cell cycle, CDKs and cancer: a changing paradigm. *Nat Rev Cancer.* 2009; 9:153-166.
 23. Freemantle SJ and Dmitrovsky E. Cyclin E transgenic mice: discovery tools for lung cancer biology, therapy, and prevention. *Cancer prevention research.* 2010; 3:1513-1518.
 24. Rosenberg E, Demopoulos RI, Zeleniuch-Jacquotte A, Yee H, Sorich J, Speyer JL and Newcomb EW. Expression of cell cycle regulators p57(KIP2), cyclin D1, and cyclin E in epithelial ovarian tumors and survival. *Human pathology.* 2001; 32:808-813.
 25. Blagosklonny MV. NCI's provocative questions on cancer: some answers to ignite discussion. *Oncotarget.* 2011; 2:1352-1367.
 26. Blagosklonny MV. Do cells need CDK2 and ... Bcr-Abl? Cell death and differentiation. 2004; 11:249-251.
 27. Valabrega G, Montemurro F and Aglietta M. Trastuzumab: mechanism of action, resistance and future perspectives in HER2-overexpressing breast cancer. *Annals of oncology : official journal of the European Society for Medical Oncology / ESMO.* 2007; 18:977-984.
 28. Pao W and Chmielecki J. Rational, biologically based treatment of EGFR-mutant non-small-cell lung cancer. *Nature reviews Cancer.* 2010; 10(11):760-774.
 29. Gray-Schopfer V, Wellbrock C and Marais R. Melanoma biology and new targeted therapy. *Nature.* 2007; 445:851-857.
 30. Druker BJ, Tamura S, Buchdunger E, Ohno S, Segal GM, Fanning S, Zimmermann J and Lydon NB. Effects of a selective inhibitor of the Abl tyrosine kinase on the growth of Bcr-Abl positive cells. *Nature medicine.* 1996; 2:561-566.
 31. Druker BJ, Talpaz M, Resta DJ, Peng B, Buchdunger E, Ford JM, Lydon NB, Kantarjian H, Capdeville R, Ohno-Jones S and Sawyers CL. Efficacy and safety of a specific inhibitor of the BCR-ABL tyrosine kinase in chronic myeloid leukemia. *The New England journal of medicine.* 2001; 344:1031-1037.
 32. Hu Q, Lu YY, Noh H, Hong S, Dong Z, Ding HF, Su SB and Huang S. Interleukin enhancer-binding factor 3 promotes breast tumor progression by regulating sustained urokinase-type plasminogen activator expression. *Oncogene.* 2013; 32:3933-3943.
 33. Su S, Li Y, Luo Y, Sheng Y, Su Y, Padia RN, Pan ZK, Dong Z and Huang S. Proteinase-activated receptor 2 expression in breast cancer and its role in breast cancer cell migration. *Oncogene.* 2009; 28:3047-3057.
 34. Hong S, Noh H, Chen H, Padia R, Pan ZK, Su SB, Jing Q, Ding HF and Huang S. Signaling by p38 MAPK Stimulates Nuclear Localization of the Microprocessor Component p68 for Processing of Selected Primary MicroRNAs. *Sci Signal.* 2013; 6:ra16.

ORIGINAL ARTICLE

Epithelial–mesenchymal transition of ovarian cancer cells is sustained by Rac1 through simultaneous activation of MEK1/2 and Src signaling pathways

D Fang^{1,2}, H Chen³, JY Zhu⁴, W Wang¹, Y Teng^{5,6}, H-F Ding⁶, Q Jing⁷, S-B Su^{1,2} and S Huang^{1,2,4}

Epithelial–mesenchymal transition (EMT) is regarded as a crucial contributing factor to cancer progression. Diverse factors have been identified as potent EMT inducers in ovarian cancer. However, molecular mechanism sustaining EMT of ovarian cancer cells remains elusive. Here we show that the presence of SOS1/EPS8/ABI1 complex is critical for sustained EMT traits of ovarian cancer cells. Consistent with the role of SOS1/EPS8/ABI1 complex as a Rac1-specific guanine nucleotide exchange factor, depleting Rac1 results in the loss of most of mesenchymal traits in mesenchymal-like ovarian cancer cells, whereas expressing constitutively active Rac1 leads to EMT in epithelial-like ovarian cancer cells. With the aid of clinically tested inhibitors targeting various EMT-associated signaling pathways, we show that only combined treatment of mitogen-activated extracellular signal-regulated kinase 1/2 (MEK1/2) and Src inhibitors can abolish constitutively active Rac1-led EMT and mesenchymal traits displayed by mesenchymal-like ovarian cancer cells. Further experiments also reveal that EMT can be induced in epithelial-like ovarian cancer cells by co-expressing constitutively active MEK1 and Src rather than either alone. As the activities of Erk and Src are higher in ovarian cancer cells with constitutively active Rac1, we conclude that Rac1 sustains ovarian cancer cell EMT through simultaneous activation of MEK1/2 and Src signaling pathways. Importantly, we demonstrate that combined use of MEK1/2 and Src inhibitors effectively suppresses development of intraperitoneal xenografts and prolongs the survival of ovarian cancer-bearing mice. This study suggests that cocktail of MEK1/2 and Src inhibitors represents an effective therapeutic strategy against ovarian cancer progression.

Oncogene advance online publication, 12 September 2016; doi:10.1038/onc.2016.323

INTRODUCTION

Ovarian cancer is the gynecological cancer with the highest mortality rate and a 5-year survival rate has been almost unchanged in the past 30 years, remaining at about 30%. High mortality rate of ovarian cancer is most likely to be caused by late diagnosis when patients are already in advanced stages.¹ Standard treatment has been surgical debulking followed by chemotherapy.² Although most patients respond initially, almost all of them will relapse and ultimately meet their demise owing to metastasis.¹ Therefore, finding ways to contain metastasis may represent effective therapeutic strategy to help ovarian cancer patient survival.

Epithelial–mesenchymal transition (EMT) is a phenomenon during which cells undergo transition from an epithelial-to-mesenchymal phenotype.³ As cancer cells acquire the ability to invade and to migrate through the process of EMT, EMT is thus recognized as a prerequisite of metastasis.^{3–5} EMT can be induced by diverse factors that include transforming growth factor β /bone morphogenetic proteins, receptor tyrosine kinases, Wnt and Notch signaling pathways.^{3–5} Recent studies have also established a strong connection between tumor microenvironment and EMT because hypoxia,^{6,7} inflammation^{8,9} and oxidation stress,¹⁰ phenomenon commonly detected in tumor microenvironment, are

potent EMT inducers. Signals triggered by these factors all converge on EMT-inducing transcriptional factors such as Snail, Slug, Twist and Zeb1/2 that diminish the expression of epithelial-related genes such as E-cadherin and, at the same time, enhance the expression of mesenchymal-related genes, such as vimentin.^{3–5}

Like other epithelial-derived tumors, extensive evidences have demonstrated EMT as a critical step for ovarian cancer progression.^{11,12} Immunohistological analyses of both primary and metastatic ovarian carcinoma reveal that EMT is significantly associated with peritoneal metastasis and survival of ovarian cancer patients.^{13,14} Correlation between EMT and aggressiveness of ovarian cancer is also supported by gene expression-based studies in which metastatic tumors generally exhibit mesenchymal signatures.^{15,16} Moreover, overexpression of EMT-inducing transcription factors like Snail, Twist and Zeb1/2 is frequently associated with poor prognosis of ovarian cancer.^{16,17} Importantly, factors provoking EMT in ovarian cancer cells generally promote ovarian cancer progression, whereas factors suppressing EMT usually hinder cancer progression. For example, mucin 4 that induces EMT in ovarian cancer cells strongly fosters cancer progression and is often overexpressed in high-grade ovary tumors.¹⁸ MicroRNA-200c that deters EMT inhibits metastasis of

¹Research Center for Traditional Chinese Medicine Complexity System, Shanghai University of Traditional Chinese Medicine, Shanghai, China; ²E-institute of Shanghai Municipal Education Committee, Shanghai University of Traditional Chinese Medicine, Shanghai, China; ³Department of Obstetrics and Gynecology, Zhongnan Hospital of Wuhan University, Wuhan, China; ⁴Department of Anatomy and Cell Biology, University of Florida College of Medicine, Gainesville, FL, USA; ⁵Department of Oral Biology, Dental College of Georgia, Augusta University, Augusta, GA, USA; ⁶Georgia Cancer Center, Augusta University, Augusta, GA, USA and ⁷Department of Cardiology, Changhai Hospital, Shanghai, China. Correspondence: S-B Su, Research Center for Traditional Chinese Medicine Complexity System, Shanghai University of Traditional Chinese Medicine, Shanghai, China or Dr S Huang, Department of Anatomy and Cell Biology, University of Florida College of Medicine, 2033 Mowry Road, PO Box 103633, Gainesville, FL 32610, USA. E-mail: shibingsu07@163.com or shuanghuang@ufl.edu

Received 31 August 2015; revised 7 June 2016; accepted 28 July 2016

CD117+CD44+ ovarian cancer stem cells.¹⁹ Another example that highlights the importance of EMT in ovarian cancer progression is that chemo-resistant ovarian cancer cells frequently display significant mesenchymal traits.²⁰ However, molecular mechanism sustaining mesenchymal phenotype of ovarian cancer cells is poorly understood.

We previously discovered that SOS1/EP8/ABI1 complex is critically associated with ovarian cancer aggressiveness.²¹ In this study, we show that sustained EMT necessitates the presence of SOS1/EP8/ABI1 complex because depleting any component of this complex resulted in the loss of EMT traits in mesenchymal-like ovarian cancer cells, whereas restoring an intact SOS1/EP8/ABI1 complex in epithelial-like ovarian cancer cells confer them with mesenchymal characteristics. Consistent with the role of SOS1/EP8/ABI1 complex as a Rac1-specific guanine nucleotide exchange factor, knockdown of Rac1 repressed EMT in mesenchymal-like ovarian cancer cells, whereas expressing constitutively active Rac1 led to the occurrence of EMT in epithelial-like ovarian cancer cells. With the aid of clinically tested small-molecule inhibitors targeting distinct EMT-associated signaling pathways, we show that the combined use of mitogen-activated extracellular signal-regulated kinase 1/2 (MEK1/2) (AZD6244) and Src inhibitors (AZD0530), but not either alone, abolished Rac1-led EMT and also suppressed mesenchymal traits displayed by mesenchymal-like ovarian cancer cells. These results raise the possibility that simultaneous activation of MEK1/2 and Src is required for sustained EMT in ovarian cancer cells. This possibility is supported by the observation that forced expression of both constitutively active MEK1 and Src, rather than either alone, led to EMT in epithelial-like ovarian cancer cells. Our data also indicate that Rac1-MEK/Src signaling pathway most likely promotes EMT by upregulating the expression of Twist and Zeb1/2. Finally, we demonstrate that cocktail of AZD6244 and AZD0530 effectively suppressed intraperitoneal xenograft development and prolonged the survival of ovary tumor-bearing mice.

RESULTS

Presence of SOS1/EP8/ABI1 complex is essential for sustained EMT in ovarian cancer cells

We previously screened a panel of established ovarian cancer cell lines for their capability to develop intraperitoneal xenograft and identified ES2, HEY, OCC1, OVCAR5 and SK-OV3 as capable lines, whereas HEC1A, IGROV1, OVCAR3 and TOV21G as incapable ones.^{21,22} Given the close correlation between the capability to develop intraperitoneal xenograft and the potential of peritoneal metastasis among ovarian cancer cells,²² we examined EMT traits of these lines by determining their E-cadherin/vimentin expression and *in vitro* invasiveness. Western blotting showed that lines with the capability to develop intraperitoneal xenografts all displayed robust level of vimentin (a mesenchymal marker) (Figure 1a) and were able to invade Matrigel gel (Figure 1b). With the exception of IGROV1, lines incapable of developing intraperitoneal xenograft expressed E-cadherin (an epithelial marker) and exhibited no detectable vimentin (Figure 1a). Moreover, these lines were unable to invade Matrigel gel (Figure 1b). These results demonstrate that lines with capability for intraperitoneal xenograft development exhibit EMT characteristics.

As we previously revealed that the presence of SOS1/EP8/ABI1 complex is critical for the development of intraperitoneal xenograft in ovarian cancer cells,²¹ we next investigated a potential functional link between EMT and SOS1/EP8/ABI1 complex by lentivirally silencing SOS1, EP8 or ABI1 in OVCAR5 and SK-OV3 cells. Western blotting showed that knockdown of any of them reduced the level of vimentin, whereas induced E-cadherin expression (Figure 1c). Matrigel invasion assay further showed that depleting any of them impaired the capability of

OVCAR5 and SK-OV3 cells to invade Matrigel (Figure 1d). In parallel experiments, we introduced ABI1 into ABI1-negative OVCAR3, EP8 into EP8-negative IGROV1 and SOS1 into SOS1-negative TOV21G cells. Their forced expression resulted in the induction of vimentin and disappearance of E-cadherin in these cells (Figure 1e). Moreover, these cells became highly invasive (Figure 1f). These results suggest that SOS1/EP8/ABI1 complex is critically linked to the sustained EMT characteristics of ovarian cancer cells.

Rac1 regulates EMT in ovarian cancer cells

SOS1/EP8/ABI1 complex is a Rac1-specific guanine nucleotide exchange factor that mediates Ras-induced Rac1 activation.²³ The observation that sustained EMT is regulated by SOS1/EP8/ABI1 complex (Figure 1) raises the possibility that Rac1 is involved in ovarian cancer cell EMT. To test this possibility, we augmented Rac1 activity in epithelial-like OVCAR3 and HEC1A cells by forcing the expression of constitutively active Rac1 (Myc-Rac1G12V) (Figure 2a and Supplementary Figure S1A). Both western blotting and immunofluorescence staining showed that expression of Rac1G12V diminished E-cadherin, whereas induced vimentin expression in both cell lines (Figures 2a and b). Upon microscopic observation, OVCAR3 and HEC1A cells with Rac1G12V expression displayed an elongated mesenchymal morphology, whereas control cells exhibited a cobble stone-like epithelial phenotype (Figure 2c). Analysis of cell shapes with the aid of Image J software (NIH, Bethesda, MA, USA) revealed that the ratio of length to width in cells with Rac1G12V expression was at least twice of that in control cells (Figure 2d). Moreover, forced expression of Rac1G12V rendered both OVCAR3 and HEC-1A lines capable of invading Matrigel (Figure 2e).

We next lentivirally introduced Rac1 short hairpin RNAs (shRNAs) into mesenchymal-like OVCAR5 and SK-OV3 cells. Knockdown of Rac1 reduced >60% of endogenous Rac1 activity judging by the amount of GTP-bound Rac1 (Supplementary Figure S1B). Western blotting and immunofluorescence staining showed that silencing Rac1 led to the induction of E-cadherin and reduction of vimentin in these cells (Figures 3a and b). Moreover, Rac1-knockdown cells exhibited an epithelial morphology while control cells displayed a mesenchymal phenotype (Figure 3c). Analysis of cell shapes revealed that ratio of length to width in Rac1-knockdown cells was reduced >50% compared with control cells (Figure 3d). Matrigel invasion assay further showed that these cells displayed greatly reduced *in vitro* invasiveness (Figure 3e). These results suggest that Rac1 has a critical role in the EMT of ovarian cancer cells.

Activation of both MEK1/2 and Src signaling pathways is required for Rac1-led ovarian cancer cell EMT

EMT can be induced by multiple signaling pathways, including transforming growth factor β , Notch, Wnt/ β -catenin, nuclear factor- κ B and receptor tyrosine kinases, either alone or in cooperation.^{8,24–28} Rac1 has also been previously reported to regulate EMT in breast cancer cells through the regulation of p21-activated kinase and reactive oxygen species.^{29,30} To determine downstream signaling pathways mediating Rac1-led EMT in ovarian cancer cells, we treated OVCAR3/Rac1G12V cells with inhibitors specific for various signaling molecules: AZD6244 for MEK1/2, LY2109761 for T β R/II kinase inhibitor, FH535 for Wnt, TPCA1 for IKK2, LY450139 for γ -secretase (Notch), FRAX597 for p21-activated kinase, Genistein for tyrosine kinase, AZD0530 for Src, N-acetyl-cysteine for reactive oxygen species, Wortmannin for phosphoinositide-3 kinase, TAK-715 for p38, and SP600125 for c-Jun N-terminal kinase (Supplementary Table S1). Among these inhibitors, AZD6244 and AZD0530 were able to partially restore E-cadherin in OVCAR3/Rac1G12V cells though they did not significantly alter the level of vimentin (Figure 4a).

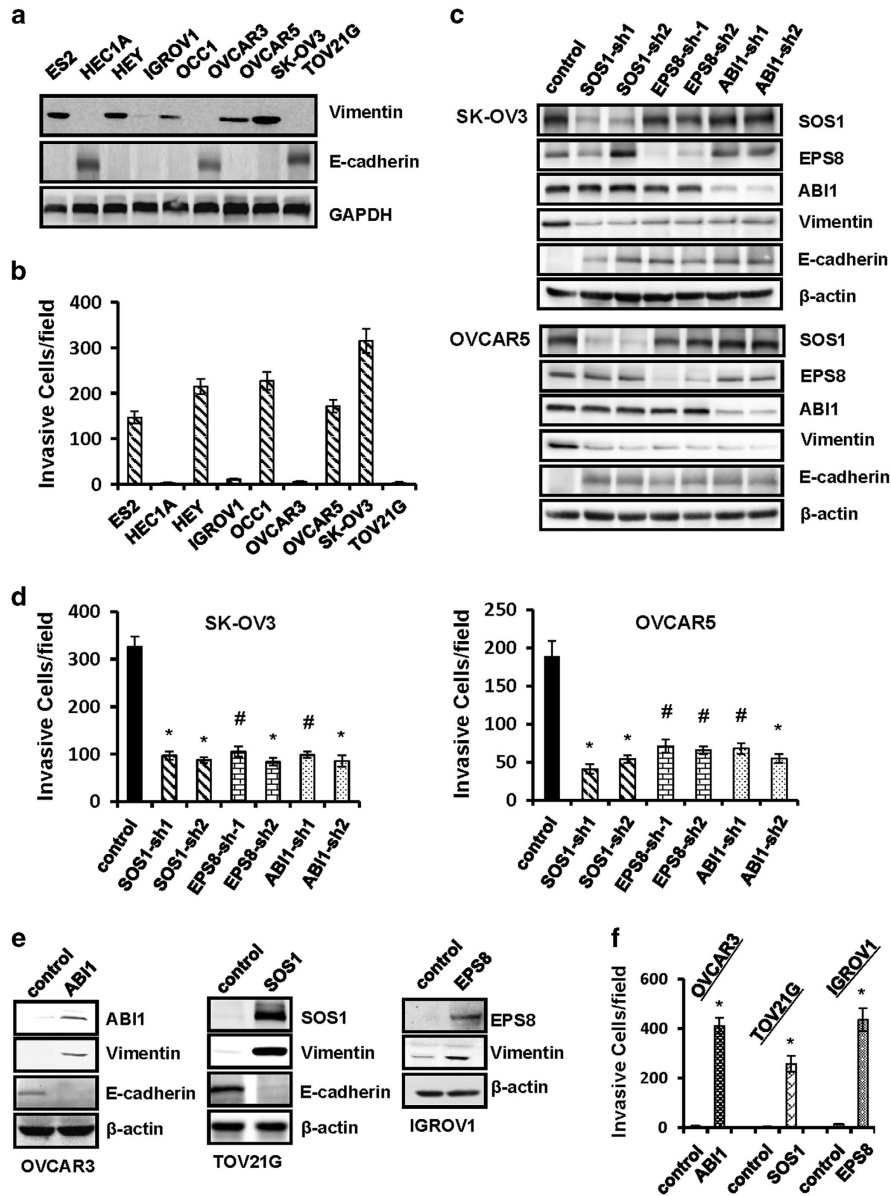


Figure 1. Presence of SOS1/EPS8/ABI1 complex is correlated with EMT in ovarian cancer cells. (a) Western blotting analysis of E-cadherin, vimentin and glyceraldehyde 3-phosphate dehydrogenase in various ovarian cancer cell lines. (b) Matrigel *in vitro* invasion assay was performed to analyze the invasiveness of various ovarian cancer cell lines. Data are means \pm s.e. ($n=4$). (c) SK-OV3 and OVCAR5 cells were transduced with lentiviral vectors containing scramble sequence, SOS1, EPS8 or ABI1 shRNA for 4 days followed by western blotting to detect SOS1, EPS8, ABI1, E-cadherin, vimentin and β -actin with the respective antibodies. (d) SK-OV3 and OVCAR5 cells were lentivirally transduced with lentiviral vectors containing scramble sequence, SOS1, EPS8 or ABI1 shRNA for 4 days followed by the analysis of *in vitro* invasiveness using Matrigel invasion chambers. Data are means \pm s.e. ($n=4$). * $P < 0.005$; # $P < 0.05$ vs control. (e) OVCAR3, TOV21G and IGROV1 cells were transduced with lentiviral vector containing ABI1, SOS1 or EPS8 expression cassette, respectively, for 4 days. Cells were then lysed and lysates subjected to western blotting to detect SOS1, EPS8, ABI1, E-cadherin, vimentin and β -actin with the respective antibodies. (f) Matrigel invasion assay to analyze the *in vitro* invasiveness of OVCAR3/ABI1, TOV21G/SOS1 and IGROV1/EPS8 cells. Data are means \pm s.e. ($n=4$). * $P < 0.005$ vs control.

Interestingly, combined treatment of AZD6244 and AZD0530 greatly enhanced the amount of both E-cadherin mRNA and protein, whereas also diminished vimentin mRNA and protein in both OVCAR3/Rac1G12V and HEC1A/Rac1G12V cells (Figures 4b and c). Microscopic analysis further showed that mesenchymal morphology of OVCAR3/Rac1G12V and HEC1A/Rac1G12V cells was reverted back to epithelial one (Figure 4d).

In subsequent experiments, we analyzed the effect of AZD6244 and AZD0530 on EMT traits of OVCAR5 and SK-OV3 cells. Quantitative reverse transcriptase-PCR (qRT-PCR) showed that

both inhibitors in individuality were able to moderately induce E-cadherin mRNA while displayed only marginal effect on vimentin mRNA (Figure 5a). In contrast, treating these cells simultaneously with both inhibitors led to much greater induction of E-cadherin mRNA and significant reduction in vimentin mRNA (Figure 5a). Similarly, western blotting showed that combined use of AZD6244 and AZD0530 led to dramatic increase in the abundance of E-cadherin and disappearance of vimentin in both lines (Figure 5b). In addition, mesenchymal morphology of OVCAR5 and SK-OV3 cells was largely changed to epithelial-like

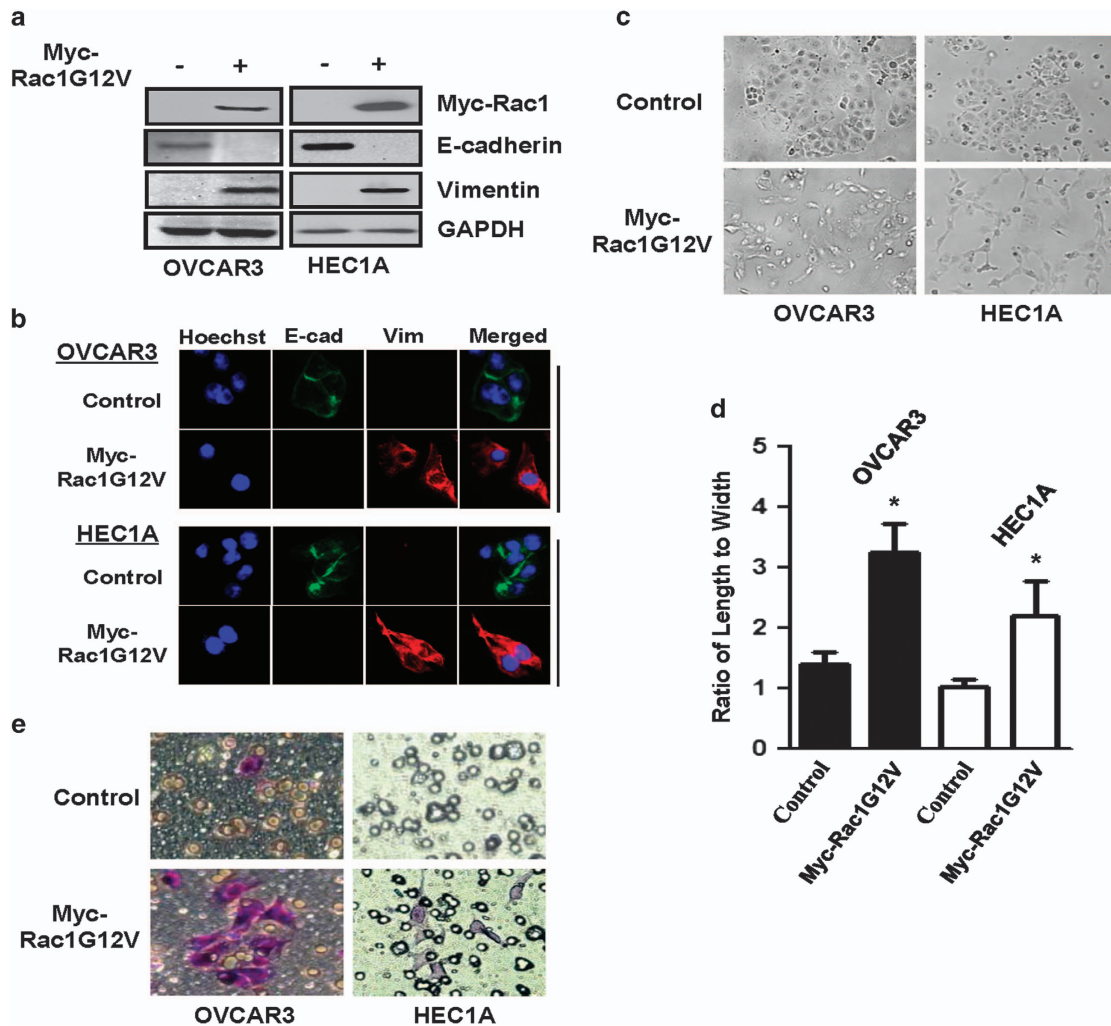


Figure 2. Constitutively active Rac1 induces EMT in ovarian cancer cells. **(a)** OVCAR3 and HEC-1A cells were lentivirally transduced with empty vector (control) or vector containing Myc-tagged Rac1G12V for 4 days. Cells were lysed and cell lysates were subjected to western blotting to detect Myc-tagged Rac1G12V, E-cadherin, vimentin and glyceraldehyde 3-phosphate dehydrogenase with the respective antibodies. **(b)** Immunofluorescence staining was performed to detect E-cadherin and vimentin in control and Rac1G12V-transduced OVCAR3 and HEC-1A cells. **(c)** Morphologies of control and Rac1G12V-transduced OVCAR3 and HEC-1A cells. **(d)** Ratio of length to width in control and Rac1G12V-transduced OVCAR3 and HEC1A cells. Data are means \pm s.e. ($n = 104$). $*P < 0.005$ vs control. **(e)** Overnight-cultured control and Rac1G12V-transduced OVCAR3 and HEC-1A cells were detached with phosphate-buffered saline containing 10 mM EDTA, then washed and plated into upper chambers of Matrigel invasion assay system for 24 h. Cells on the undersurface of upper chambers were stained with crystal solution and visualized under a phase-contrast microscope.

one upon the combined treatment of AZD6244 and AZD0530 (Figure 5c). Moreover, combined treatment of AZD6244 and AZD0530 greatly slowed the rate of both lines to fill the gap in wound-healing assay (Figure 5d) and also inhibited cell migration measured by Transwell assay (Figures 5e and f). Taken together, these results suggest that Rac1-led EMT requires the activation of both MEK1/2 and Src signaling pathways.

Simultaneous activation of MEK1 and Src is sufficient to induce EMT. To further link MEK1/2 and Src signaling pathways to Rac1-led EMT, we analyzed the activation status of MEK1/2 and Src signaling pathways through the detection of extent of Erk and Src phosphorylation. Western blotting revealed that levels of phosphorylated Erk and Src were much higher in Rac1G12V-expressing OVCAR3 and HEC1A cells than their respective control cells (Figure 6a). In a parallel experiment, we also observed that knockdown of Rac1 led to a dramatic reduction in the levels of phosphorylated Erk and Src in SK-OV3 and OVCAR5 cells

compared with control (Figure 6b). These results indicate that Rac1 activation leads to higher activities of MEK1/2 and Src signaling pathways. As activation of MEK/Erk can be downstream of Src and vice versa, we tested the effect of AZD0530 (blocking Src) on phosphor-Erk and AZD6244 (blocking MEK1/2) on phosphor-Src in OVCAR3/Rac1G12V cells. Western blotting showed that AZD0530 blocked Src phosphorylation but did not alter the level of phosphor-Erk (Supplementary Figure S2). Similarly, AZD6244 diminished Erk phosphorylation while displayed no effect on the abundance of phosphorylated Src (Supplementary Figure S2). These results not only confirm the specificities of these inhibitors but also indicate that Rac1 activates MEK1/2 and Src signaling pathways in parallel rather than sequentially.

We next introduced constitutively active MEK1 (MEK1-DD) and Src (Src-Y527F) into OVCAR3 or HEC1A cells individually or together. Forced expression of either MEK1-DD or Src-Y527F mutant slightly decreased E-cadherin, whereas moderately increased the amount of vimentin in both lines (Figures 6c

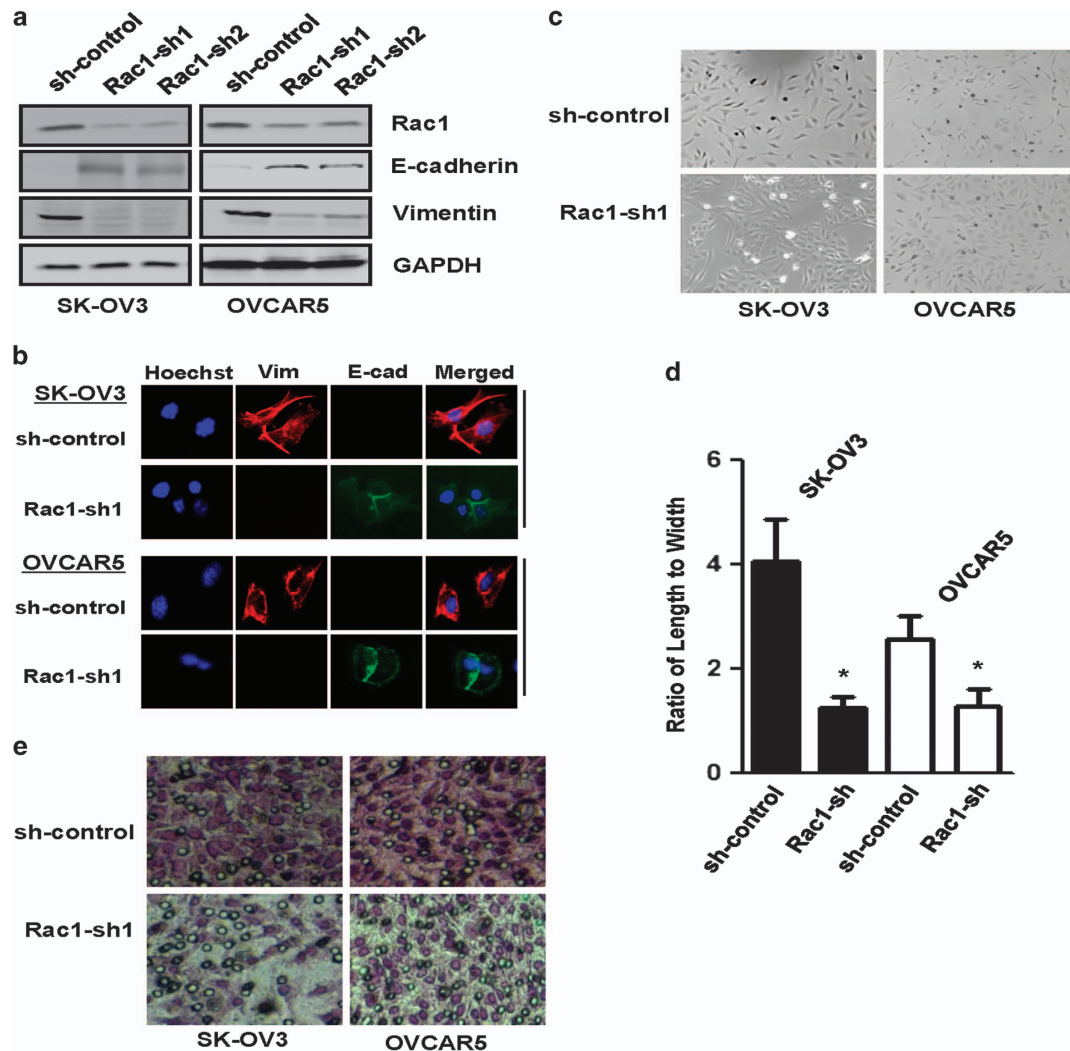


Figure 3. Knockdown of Rac1 leads to the suppression of EMT in ovarian cancer cells. **(a)** SK-OV3 and OVCAR5 cells were transduced with lentiviral vectors containing scramble sequence or Rac1 shRNA for 4 days followed by western blotting to detect Rac1, E-cadherin, vimentin and glyceraldehyde 3-phosphate dehydrogenase with the respective antibodies. **(b)** Immunofluorescence staining of E-cadherin and vimentin of control and Rac1-knockdown SK-OV3 and OVCAR5 cells. **(c)** Morphologies of control and Rac1-knockdown SK-OV3 and OVCAR5 cells. **(d)** Ratio of length to width in control and Rac1-knockdown SK-OV3 and OVCAR5 cells. Data are means \pm s.e. ($n = 111$). * $P < 0.005$ vs control. **(e)** *In vitro* invasion of control and Rac1-knockdown SK-OV3 and OVCAR5 cells.

and d). However, simultaneously expressing both MEK1-DD and Src-Y527F mutants markedly diminished E-cadherin, whereas caused a robust vimentin expression (Figures 6c and d). These results are clearly consistent with the notion that concerted action of MEK1/2 and Src signaling pathways downstream of Rac1 facilitates EMT in ovarian cancer cells. Moreover, we observed that OVCAR3 and HEC1A cells co-expressing MEK1-DD and Src-Y527F were highly migratory, whereas their respective control cells were little migratory as measured by Transwell assay (Figure 6e). Microscopic observation also indicated the occurrence of EMT in OVCAR3 and HEC1A cells co-expressing MEK1-DD and Src-Y527F as they exhibited typical mesenchymal morphology (Figure 6f).

Activities of MEK1/2 and Src are critical for upregulation of Twist and Zeb1/2 in ovarian cancer cells. To further elucidate molecular mechanism underlying Rac1-led EMT, we performed an expression array to assess the change in the levels of 84 EMT-associated genes using total RNA isolated from control and Rac1G12V-expressing OVCAR3 cells. Compared with the control, 29 genes increased, 22 decreased and 35 unchanged in OVCAR3/Rac1G12V

cells (Supplementary Table S2). Level of E-cadherin (CDH1) was found to be decreased by 64-fold, whereas vimentin (Vim) increased >32 -fold in OVCAR3/Rac1G12V cells when compared with the control (Supplementary Table S2), consistent with the change in their protein abundance detected by western blotting (Figure 2a). Further assessment of genes in which their expression was altered also revealed that the levels of Twist, Zeb1 and Zeb2, three key EMT-inducing transcription factors, were much higher in OVCAR3 or HEC1A cells expressing Rac1G12V when compared with the control (Supplementary Table S2, Figure 7a and Supplementary Figure S3A). Subsequent analysis also showed that amount of Twist, Zeb1 and Zeb2 mRNA was increased by the expression of MEK1-DD or Src-527D and in much greater extent by them together (Figure 7b and Supplementary Figure S3B). In addition, analysis of established ovarian cancer cell lines revealed that Twist, Zeb1 and Zeb2 mRNA were generally higher in mesenchymal-like ovarian cancer cell lines than in epithelial-like ones (Figure 7c).

To investigate the importance of MEK1/2 and Src signaling pathways in Twist and Zeb1/2 expression, we treated

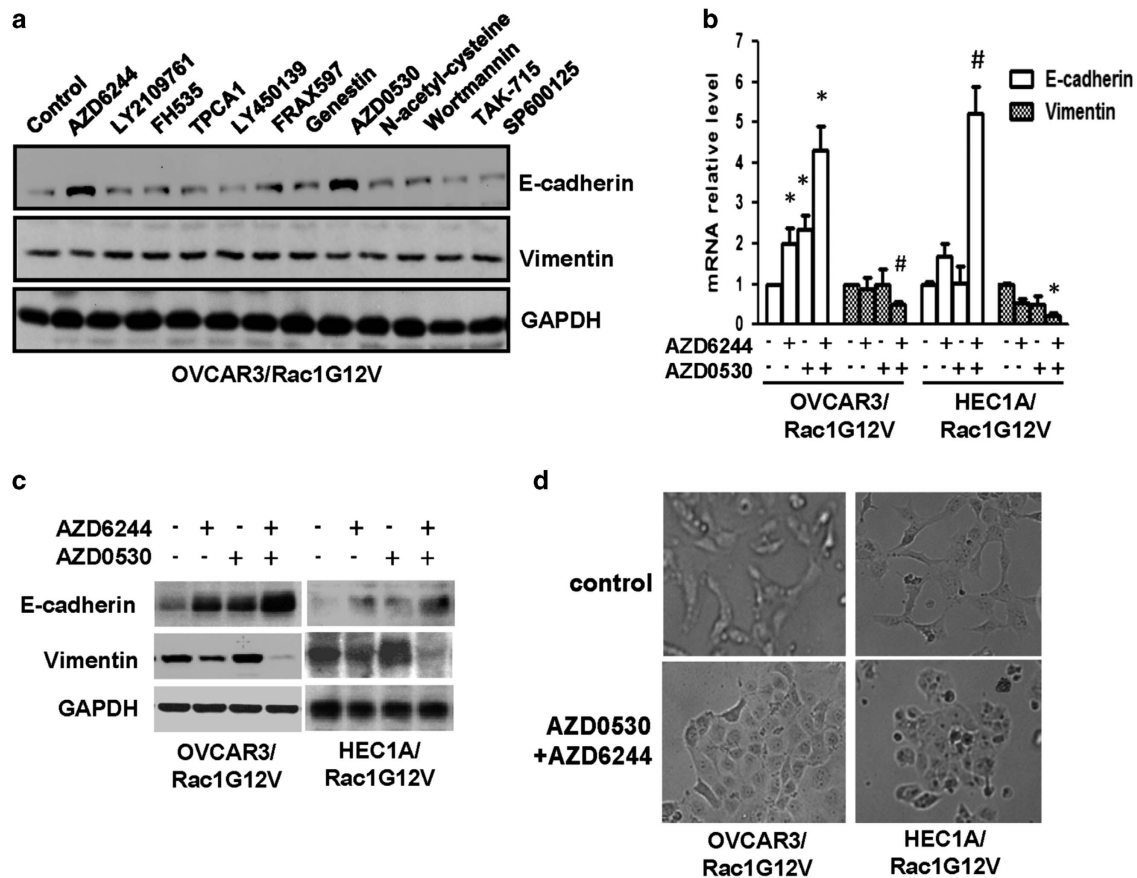


Figure 4. Rac1-led EMT depends on the activities of MEK1/2 and Src. (a) OVCAR3/Rac1G12V cells were treated with various inhibitors for 3 days, then lysed and cell lysates were subjected to western blotting to detect E-cadherin, vimentin and glyceraldehyde 3-phosphate dehydrogenase (GAPDH) with the respective antibodies. (b) OVCAR3/Rac1G12V and HEC1A/Rac1G12V cells were treated with 0.5 μM AZD0530 or 5 μM AZD6244 alone or together for 3 days, total RNA was then extracted and qRT-PCR was performed to determine the levels of E-cadherin, vimentin and β -actin mRNA. Data are means \pm s.e. ($n = 3$). * $P < 0.005$ vs vehicle control; # $P < 0.01$ vs vehicle control. (c) OVCAR3/Rac1G12V and HEC1A/Rac1G12V cells were treated with 0.5 μM AZD0530 or 5 μM AZD6244 alone or together for 3 days, then lysed and cell lysates were subjected to western blotting to detect E-cadherin, vimentin and GAPDH with the respective antibodies. (d) Morphologies of OVCAR3/Rac1G12V and HEC1A/Rac1G12V cells treated with vehicle or combination of AZD0530 and AZD6244 for 3 days.

OVCAR3/Rac1G12V and SK-OV3 cells with AZD6244 and AZD0530 either alone or together. QRT-PCR showed that levels of Twist, Zeb1 and Zeb2 mRNA were moderately decreased by MEK1/2 inhibitor AZD6244 but little altered by Src inhibitor AZD0530 (Figure 7d). In contrast, combined treatment of AZD6244 and AZD0530 greatly downregulated the expression of all three transcription factors (Figure 7d). Taken together, these results implicate that upregulation of Twist and Zeb1/2 is at least one of the contributing factors for Rac1-MEK/Src signaling axis-led EMT in ovarian cancer cells.

Combined use of MEK and Src inhibitors inhibits intraperitoneal xenograft development and prolongs the survival of ovary tumor-bearing mice

The observation that the combined use of AZD6244 and AZD0530 blocked EMT in ovarian cancer cells prompted us to investigate the efficacy of these two inhibitors to suppress ovarian cancer cell invasion. Matrigel invasion assay showed that either inhibitor alone was able to inhibit the ability of OVCAR3/Rac1G12V and SK-OV3 cells to invade Matrigel and the combined use almost completely abrogated invasion (Supplementary Figure S4). To determine their effect on ovary tumor development, female athymic nude mice were intraperitoneally injected with luciferase-expressing OVCAR3/Rac1G12V or SK-OV3 cells for 12 days

followed by orally administering AZD6244 and AZD0530 either alone or together to animals (Figure 8a). Bioluminescence imaging showed that intraperitoneal xenografts could be detected 12 days after tumor cell injection (Figure 8b). Tumors propagated rapidly in mice injected with OVCAR3/Rac1G12V cells (Figure 8b) and mice died between 4 and 5 weeks (Figure 8c). Efficient intraperitoneal xenograft development was also observed in mice receiving SK-OV3 cells (Figure 8b). The earliest morbidity of mice receiving SK-OV3 cells occurred between 2 and 3 weeks and all mice died within 8 weeks (Figure 8c). Administering AZD0530 alone to mice injected with OVCAR3/Rac1G12V cells did not significantly inhibit tumor propagation or prolong the survival ($P = 0.78$) while it was moderately effective in decreasing tumor burden and prolonging survival of mice receiving SK-OV3 cells ($P < 0.05$; Figures 8b and c). In contrast, administering AZD6244 alone significantly deterred tumor propagation and increased the lifespan of mice receiving either OVCAR3/Rac1G12V or SK-OV3 cells ($P < 0.01$; Figures 8b and c). When AZD0530 and AZD6244 were simultaneously given to animals, tumor progression was suppressed much more effectively than using either inhibitor alone ($P < 0.001$; Figure 8b). Animals receiving both AZD0530 and AZD6244 also survived significantly longer ($P < 0.001$; Figure 8c). To link deterred intraperitoneal xenograft development to blocked MEK/Src signaling and EMT, we performed immunohistochemistry to examine the intensity of phosphorylated Erk1/2,

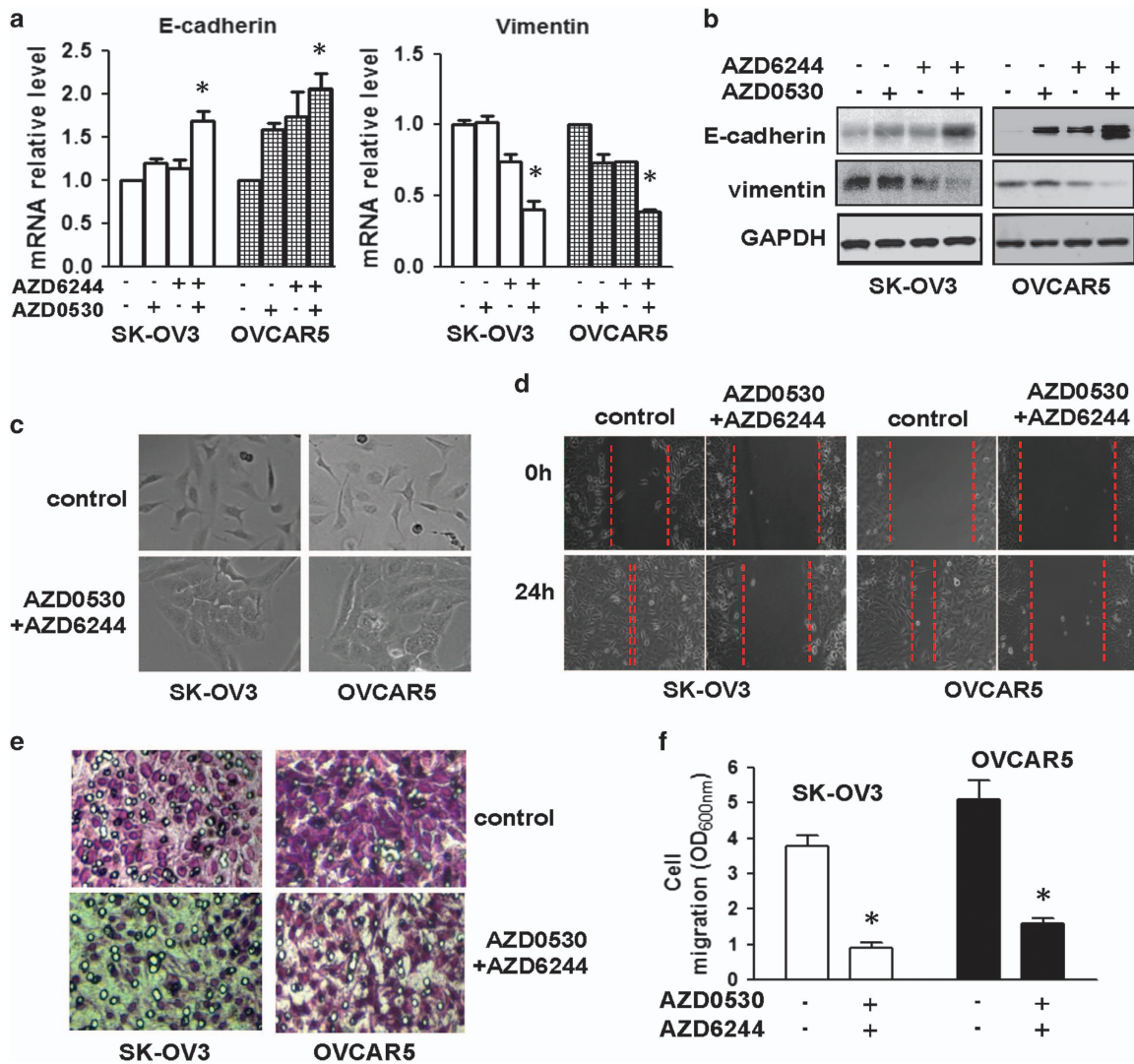


Figure 5. Sustained EMT in ovarian cancers necessitates the activity of MEK1/2 and Src. **(a)** SK-OV3 and OVCAR5 cells were treated with 0.5 μM AZD0530 or 5 μM AZD6244 alone or together for 3 days, total RNA was then isolated and qRT-PCR was performed to determine the levels of E-cadherin, vimentin and β -actin mRNA. Data are means \pm s.e. ($n = 3$). * $P < 0.01$ vs vehicle control. **(b)** SK-OV3 and OVCAR5 cells were treated with 0.5 μM AZD0530 or 5 μM AZD6244 alone or together for 3 days, then lysed and cell lysates were subjected to western blotting to detect E-cadherin, vimentin and glyceraldehyde 3-phosphate dehydrogenase with the respective antibodies. **(c)** Morphologies of SK-OV3 and OVCAR5 cells treated with vehicle or combination of AZD0530 and AZD6244 for 3 days. **(d)** SK-OV3 and OVCAR5 were grown to confluent monolayer cells in the presence or absence of AZD0530/AZD6244 for 3 days. A scratch was made with a fine pipette tip and the dislodged cells were washed away with serum-free medium. The cells were fed with medium containing 1% fetal calf serum with or without AZD0530/AZD6244, and images were taken at 0 and 24 h under a phase-contrast microscope. **(e)** SK-OV3 and OVCAR5 cells were treated with vehicle or combination of AZD0530 and AZD6244 for 3 days followed by the analysis of cell migration using Transwells. Cells that remained on the undersurface of Transwells were stained with crystal violet and visualized under a phase-contrast microscope. **(f)** Stained cells on undersurface of Transwells were solubilized and read at wavelength of 600 nm on a microplate reader. Data are means \pm s.e. ($n = 4$). * $P < 0.005$ vs control.

phosphorylated Src, E-cadherin and vimentin staining on collected tumors. Strong phosphor-Src, phosphor-Erk and vimentin but no E-cadherin staining were detected in tumors derived from OVCAR3/Rac1G12V and SK-OV3 cells (Figure 8d). Tumors derived from mice administered with AZD0530 or AZD6244 were negative for phosphor-Src and phosphor-Erk staining, respectively (Figure 8d), confirming their ability to target intended pathways. Compared with control, tumors derived from AZD0530 or AZD6244 treatment group also displayed much less vimentin staining (Figure 8d). Interestingly, E-cadherin staining was only observed in mice treated with both AZD0530 and AZD6244 (Figure 8d). These results suggest that upregulation of vimentin and downregulation of E-cadherin in ovary tumors depend on

simultaneous activation of both MEK1/2 and Src signaling pathways, thus supporting the notion that deterred tumor progression and prolonged survival of tumor-bearing mice by AZD0530 and AZD6244 are likely to be the consequence of their suppressive effect on EMT.

DISCUSSION

Role of EMT in ovarian cancer malignancies is supported by the findings that mesenchymal-like gene expression signature is generally associated with aggressive and metastatic ovarian cancer.^{13,14} It is also backed by the findings that factors inducing EMT often act as metastasis promoters.¹¹ Here we observed that

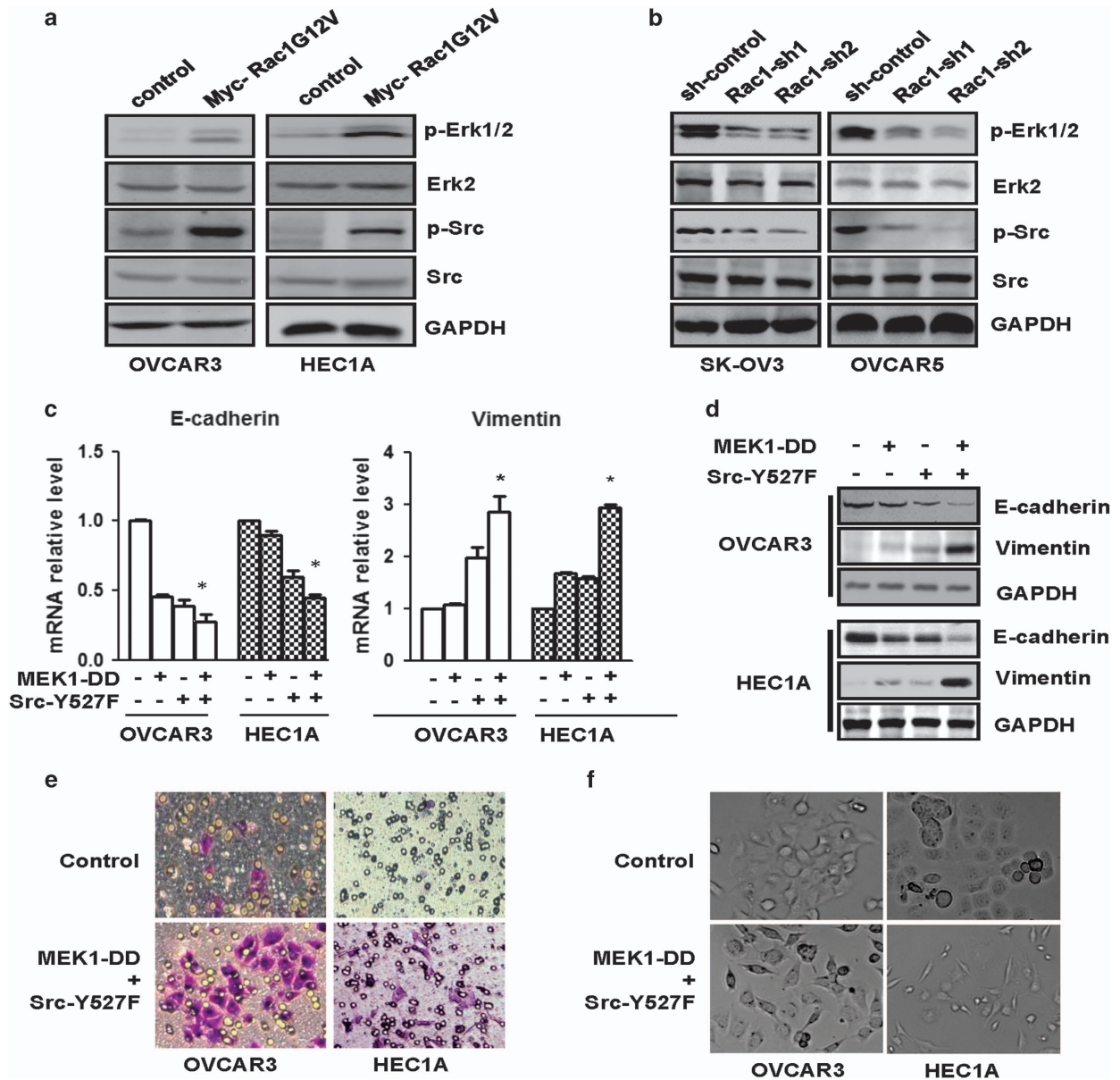


Figure 6. Simultaneous activation of MEK1/2 and Src pathways leads to EMT in ovarian cancer cells. **(a)** OVCAR3/Rac1G12V and HEC1A/Rac1G12V cells were lysed, and the cell lysates were subjected to western blotting to detect p-Erk1/2, Erk2, p-Src, Src and glyceraldehyde 3-phosphate dehydrogenase (GAPDH) using the respective antibodies. **(b)** Control and Rac1-knockdown SK-OV3 and OVCAR5 cells lysed, and the cell lysates were subjected to western blotting to detect p-Erk1/2, Erk2, p-Src, Src and GAPDH using the respective antibodies. **(c)** OVCAR3 and HEC1A cells were transduced with lentiviral vector encoding MEK1-DD or Src-Y527F individually or together for 4 days. Total RNA was extracted from these cells and then subjected to qRT-PCR to analyze the levels of E-cadherin, vimentin and β -actin mRNA. Data are means \pm s.e. ($n = 4$). $*P < 0.01$ vs control. **(d)** OVCAR3 and HEC1A cells transduced with lentiviral vector encoding MEK1-DD or Src-Y527F individually or together were lysed, and the cell lysates were subjected to western blotting to detect E-cadherin, vimentin and GAPDH with the respective antibodies. **(e)** OVCAR3 and HEC1A cells transduced with empty vector or together with vectors containing MEK1-DD and Src-Y527F were analyzed for their *in vitro* invasiveness using Matrigel invasion chambers. Cells that remained on the undersurface of invasion chambers were stained and visualized under a phase-contrast microscope. **(f)** Morphologies of OVCAR3/Rac1G12V and HEC1A/Rac1G12V cells treated with vehicle or combination of AZD0530 and AZD6244 for 3 days.

ovarian cancer cell lines capable of developing intraperitoneal xenografts are mesenchymal in nature, whereas lines incapable of developing intraperitoneal xenografts exhibited epithelial-like phenotype (Figure 1). We previously discovered that the presence of SOS1/EP8/ABI1 complex is critical for development of intraperitoneal xenografts of ovarian cancer cells.²¹ In this study, we detected that ovarian cancer cell lines with an intact SOS1/EP8/ABI1 complex all displayed EMT traits and disrupting SOS1/EP8/ABI1 complex by depleting mem-

bers of this complex led to the suppression of EMT in mesenchymal-like ovarian cancer cells, whereas restoring an intact SOS1/EP8/ABI1 complex converted epithelial-like ovarian cancer cells to mesenchymal-like ones (Figure 1). Given a close correlation between capability of intraperitoneal xenograft development and metastatic potential in ovarian cancer cells, our data suggest that SOS1/EP8/ABI1 complex may control ovarian cancer metastasis by sustaining EMT in ovarian cancer cells.

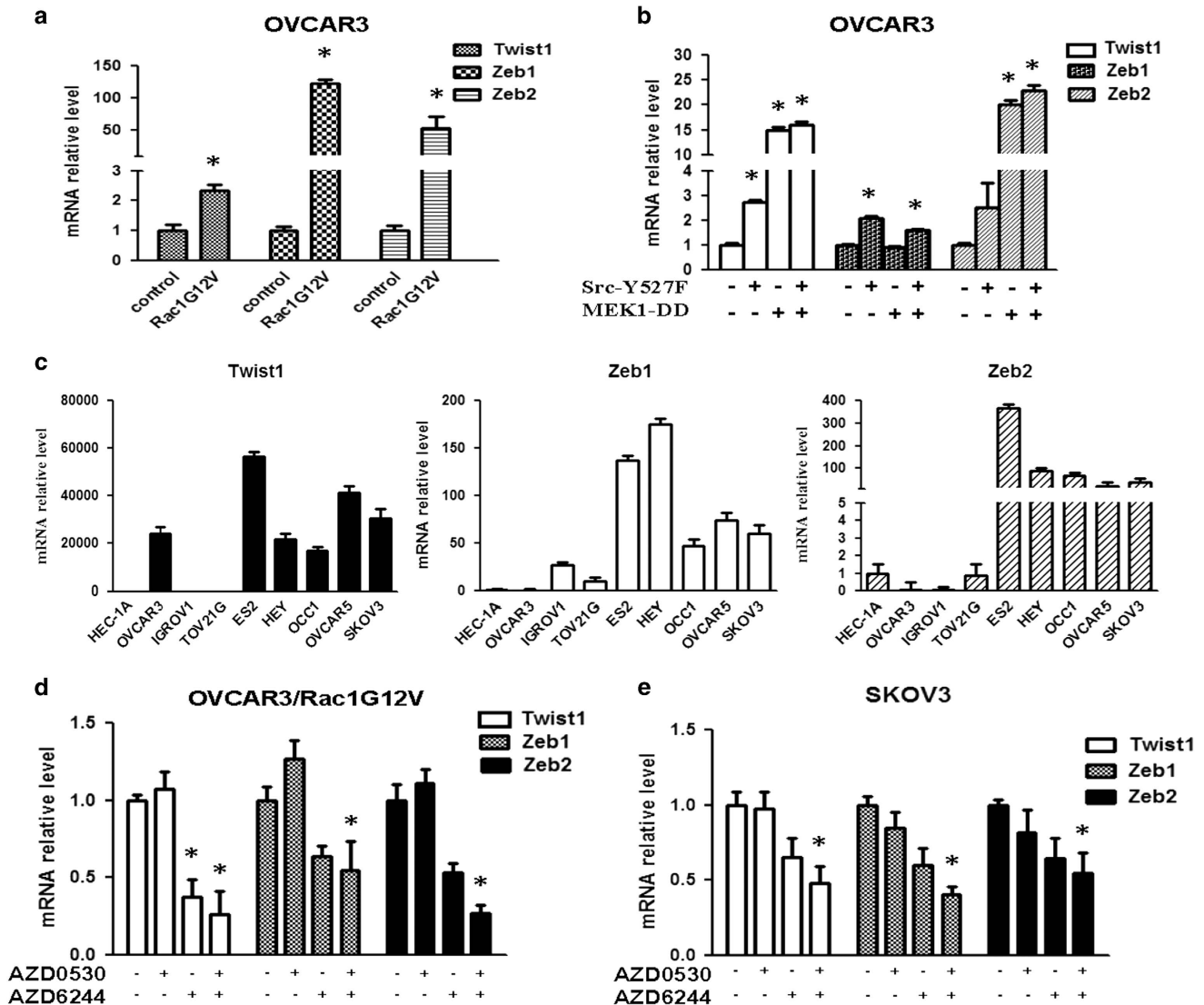


Figure 7. Rac1-MEK/Src signaling axis promotes the expression of Twist1 and Zeb1/2 in ovarian cancer cells. **(a)** qRT-PCR analysis of Twist, Zeb1 and Zeb2 in OVCAR3/Rac1G12V cells. Data are means \pm s.e. ($n = 3$). $*P < 0.05$ vs control. **(b)** qRT-PCR analysis of Twist, Zeb1 and Zeb2 in OVCAR3 cells transduced with MEK1-DD and Src-Y527F individually or together. Data are means \pm s.d. ($n = 3$). $*P < 0.05$ vs control. **(c)** qRT-PCR analysis of Twist, Zeb1 and Zeb2 in various ovarian cancers. Data are means \pm s.d. ($n = 3$). **(d)** OVCAR3/Rac1G12V cells were treated with 0.5 μ M AZD0530 or 5 μ M AZD6244 alone or together for 3 days. Cells were extracted for total RNA and total RNA was subjected to qRT-PCR to measure the levels of Twist, Zeb1 and Zeb2 mRNA. Data are means \pm s.d. ($n = 3$). $*P < 0.05$ vs vehicle. **(e)** SK-OV3 cells were treated with 0.5 μ M AZD0530 or 5 μ M AZD6244 alone or together for 3 days. Cells were extracted for total RNA and total RNA was subjected to qRT-PCR to measure the levels of Twist, Zeb1 and Zeb2 mRNA. Data are means \pm s.d. ($n = 3$). $*P < 0.05$ vs vehicle.

SOS1/EPS8/ABI1 complex is a guanine nucleotide exchange factor specifically activating Rac1.²³ The importance of SOS1/EPS8/ABI1 complex in ovarian cancer cell EMT indicates that this complex may regulate EMT through Rac1. Rac1 has been shown to participate in EMT of diverse cancer cell types. For example, Rac1 mediates EMT induced by IRGM1 in melanoma cells,³¹ interferon regulatory factor 4 binding protein in breast cancer cells³² and Twist in head and neck squamous carcinoma cells.³³ In this study, we showed that silencing Rac1 diminished EMT characteristics of mesenchymal-like ovarian cancer cells, whereas ectopically expressing constitutively active Rac1 resulted in EMT in epithelial-like ovarian cancer cells (Figures 2 and 3). These findings strongly implicate Rac1 as an EMT executor in ovarian cancer cells. A recent study reported that Rac1 overexpression was closely associated with advanced stage of ovarian cancer and poor prognosis.³⁴ We previously found that blocking Rac1 activity with

dominant-negative Rac1 suppressed intraperitoneal xenograft development.²¹ These observations are evidently in agreement with the notion that Rac1 impacts ovarian cancer progression and metastasis by promoting EMT. Several recent studies indicate the potential role of RhoA/RhoC in ovarian cancer EMT. For instance, bone morphogenetic protein 4, which induces EMT in ovarian cancer cells, also activates RhoA.³⁵ Soft matrices increased ovarian cancer malignancy by facilitating EMT in a RhoA-dependent mechanism.³⁶ Moreover, ectopic RhoC expression was shown to induce EMT in ovarian cancer cells and its presence appears to be important for growth factor-induced EMT.³⁷ It will be of great interest to investigate whether Rho facilitates ovarian cancer EMT in a similar mechanism as we identified for Rac.

Diverse signaling pathways have been linked to EMT in various cancer cell types.³⁻⁵ With the aid of specific inhibitors, we found that deterrence of EMT requires simultaneous inhibition of both

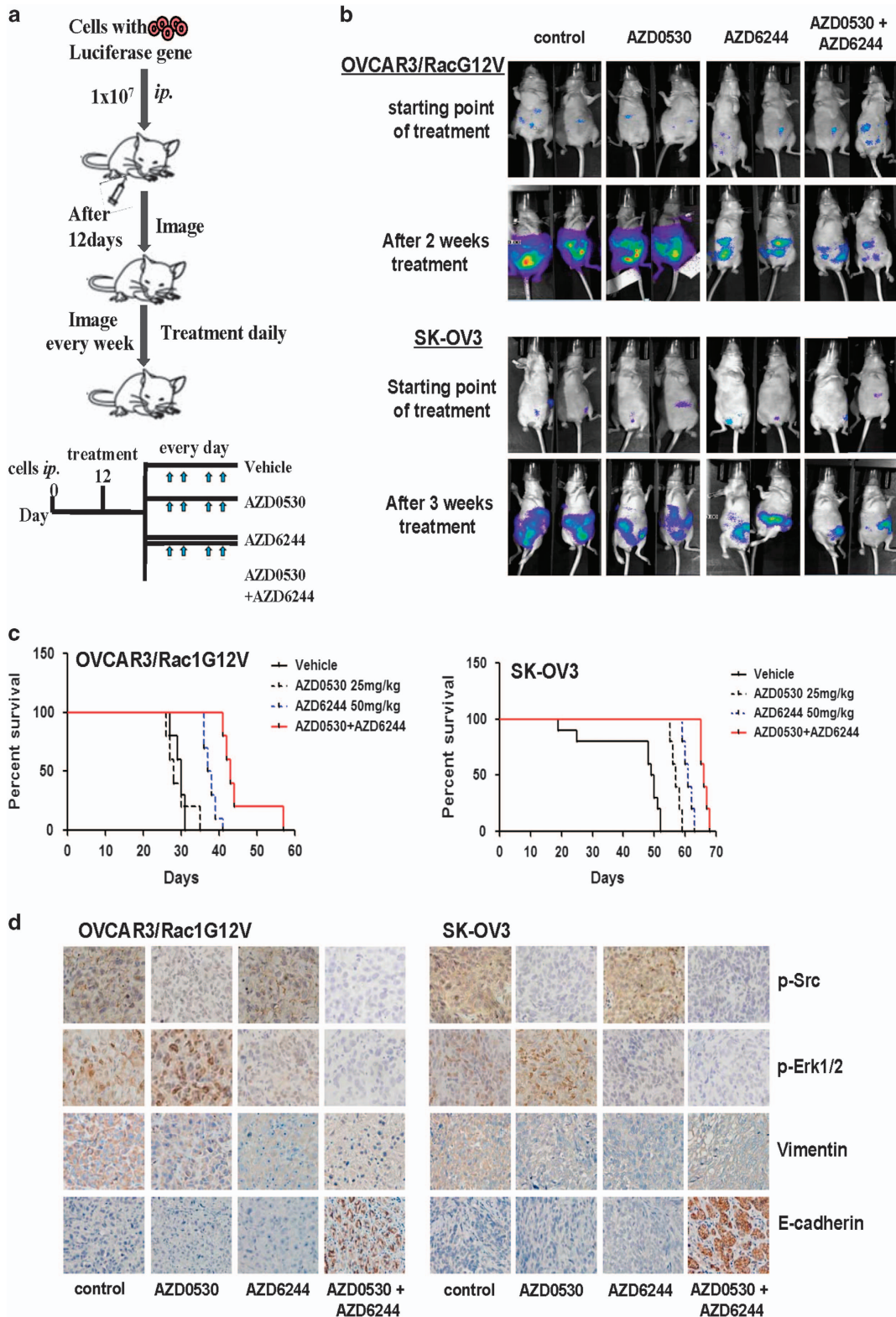


Figure 8. Combined use of MEK1/2 AND Src inhibitors suppresses ovarian cancer progression. **(a)** Flow chart of therapy scheme. **(b)** OVCAR3/Rac1V12G or SK-OV3 cells (1×10^7 cells/mouse) were injected intraperitoneally to nude mice for 12 days followed by administration of 50 mg/kg AZD6244 or 25 mg/kg AZD0530 individually or together. Tumors were imaged in Xenogen system. **(c)** Kaplan–Meier analysis of animal end point survival following treatment with AZD6244 or AZD0530 individually or in combination. **(d)** Representative pictures of immunohistochemical staining of phosphor-Src, phosphor-Erk, E-cadherin and Vimentin in tumor tissues. Scale bars, 50 μ m.

MEK1/2 and Src signaling pathways in constitutively active Rac1-expressing epithelial-like or established mesenchymal-like ovarian cancer cells (Figures 4, 5 and 7). We further showed that expressing constitutively active MEK1 and Src together, rather than either alone, led to the occurrence of EMT in epithelial-like ovarian cancer cells (Figures 6 and 7; Supplementary Figure S3). A recent study showed that Src inhibitor (AZD0530) was able to restore E-cadherin expression in at least some ovarian cancer cell lines.³⁸ Another study reported that tissue transglutaminase induced ovarian cancer cell EMT in a Src-dependent mechanism.³⁹ Moreover, CrkL was reported to regulate C-C motif chemokine ligand 19/C-C motif chemokine receptor 7-induced ovarian cancer cell EMT via MEK1/2 signaling pathway.⁴⁰ Although results from these studies pinpoint the importance of MEK1/2 and Src signaling pathway in ovarian cancer EMT, we are the first to demonstrate that a complete ovarian cancer cell EMT is actually sustained by the simultaneous activation of both MEK1/2 and Src signaling pathways downstream of Rac1.

Through the analyses of clinical specimens, activation of MEK1/2 and Src signaling pathways has been found to be associated with EMT features and disease progression of various cancer types. For instance, EMT features (increased vimentin/fibronectin and decreased E-cadherin) were found to be associated with the elevated level of activated Erk in surgical resected pancreatic tumor specimens and are the prognostic indicator for poor survival.⁴¹ In clinical head and neck squamous carcinoma specimens, level of activated Src was shown to negatively correlate with E-cadherin expression but positively associate with the abundance of vimentin and aggressive tumor characteristics.⁴² Although the association between EMT and activation status of MEK1/2 and Erk signaling pathways has not been investigated in clinical ovarian tumor specimens, our results generated from multiple established ovarian cancer cell lines and these previous findings with other cancer types strongly support the existence of such correlation in ovary tumors.

The well-recognized importance of EMT in cancer progression implicate that interfering with Rac1 activity may represent an effective strategy to suppress ovary tumorigenesis. This possibility is supported by earlier finding that dominant-negative Rac1 completely abolished intraperitoneal xenograft development of ovarian cancer cells.²¹ Unfortunately, strategy of directly targeting Rac1 is currently unavailable because efforts on developing clinically applicable Rac1 inhibitor have not been successful.⁴³ Our current study shows that Rac1 promotes EMT through simultaneous activation of MEK1/2 and Src signaling pathways. We thus reason that we may achieve the goal of interfering with Rac1 function by simultaneously targeting MEK1/2 and Src. Such strategy is apparently very feasible because of the availability of MEK1/2 and Src inhibitors that are already in phase II clinical trials. Our reasoning is evidently supported by our observation that combined use of MEK1/2 (AZD6244) and Src inhibitors (AZD0530) suppressed metastatic colonization of ovarian cancer cells and prolonged the survival of mice bearing ovary tumors (Figure 8). In conclusion, our study has laid a foundation on using currently available MEK1/2 and Src inhibitors to treat advanced ovary tumors.

MATERIALS AND METHODS

Cells, shRNAs and other reagents

All cells were maintained in Dulbecco's modified Eagle's medium containing 10% fetal bovine serum at 37 °C in a humidified incubator supplied with 5% CO₂. The shRNA sequences for Rac1 were designed using web-based Block-iT program (Life Technologies, Carlsbad, CA, USA) and subcloned into pLV-shRNA vector (Biossetta, San Diego, CA, USA). Expression and shRNA constructs for EPS8, ABI1 and SOS1 were described previously.²¹ Expression vectors for MEK1-DD and Src-Y527F were purchased from Addgene (Cambridge, MA, USA) and the coding sequences for MEK1-

DD and Src-Y527F were subcloned into lentiviral expression vector pCDH (System Biosciences, Mountain View, CA, USA). All inhibitors were purchased from commercial sources and described in Supplementary Table S1. Information for Rac1 shRNA sequences, primer sequences for PCR and antibodies are included in Supplementary Information.

Western blotting analysis

Cells in monolayer were washed with phosphate-buffered saline and harvested with radio-immunoprecipitation assay lysis buffer. Cell lysates were electrophoresed on 10–12% sodium dodecyl sulfate-polyacrylamide gels, then transferred onto nitrocellulose membranes and membranes were incubated overnight at 4 °C with primary antibodies. After several washes, membrane were incubated with horseradish peroxidase-conjugated secondary antibodies for 1 h at room temperature and developed with the SuperSignal West Femto Kit (ThermoFisher Scientific, Waltham, MA, USA).

Immunofluorescence staining and cell shape analysis

Cells seeded on coverslips were washed with ice-cold phosphate-buffered saline and then blocked with 5% heat-denatured bovine serum albumin. After membrane permeabilization with 0.5% Triton-X100, cells were stained using anti-E-cadherin monoclonal antibody or anti-vimentin polyclonal antibody followed by fluorescein or rhodamine-conjugated secondary antibodies for another hour. Nuclei were visualized by staining with 4',6-diamidino-2-phenylindole. The fluorescence staining was observed with the aid of a fluorescence microscope (Axiovert 200M; Carl Zeiss, Thornwood, NY, USA). To analyze cell shape, both length and width cell size (length:width ratio) was measured using the Image J software in >100 cells. Cell length was defined by the longest distance between any two points of the cell, and cell width was measured as the longest line perpendicular to the cell-length line.

In vitro invasion and cell migration assay

In vitro invasion assay was performed using Matrigel invasion chambers (Cell Biolabs, San Diego, CA, USA) as previously described.^{21,44,45} Briefly, 2×10^5 cells were plated into each of invasion chamber and medium containing 10% fetal calf serum was added into lower chamber. Cells were allowed to invade for 24 h followed by removing remaining cells in the invasion chambers by cotton swab. Cells on the undersurface of invasion chambers were stained with crystal violet and counted under a phase-contrast microscope. Cell migration was measured with the aid of Transwells (8.0 mm pore size) as described previously.^{46–48} Briefly, the undersurface of Transwell was coated with 10 µg/ml of collagen I and serum-free medium was added to lower chambers. Serum-starved cells (10^5 cells in 100 µl/well) were first treated with 5 µM AZD6244 and 0.5 µM AZD0530 either alone or together for 24 h, then added to Transwells and allowed to migrate for 24 h. Cells that remained in Transwells were removed with cotton swabs, and cells that attached on undersurface were stained with crystal violet solution for visualization. To quantitate cell migration, stained cells on the undersurface were solubilized with 10% acetic acid and measured at 600 nm on a Bio-Rad microplate reader (Hercules, CA, USA).

Rac1 activity assay

Rac activity assay was determined using the G-LISA Rac1 Activation Assay Kit (Cytoskeleton, Denver, CO, USA) according to the manufacturer's instructions. Briefly, overnight cultured cells were lysed and the cell lysates were used to measure Rac1 activity on an enzyme-linked immunosorbent assay-formatted and colorimetric-based assay.

Real-time PCR-based microarray assay and qRT-PCR

Effect of constitutively active Rac1 on the expression of genes associated with EMT was analyzed using human EMT RT2 Profiler PCR Array (Qiagen, Frederick, MD, USA). Total RNA isolated from control OVCAR3 and OVCAR3/Rac1V12 cells was used for screening as per the manufacturer's instructions. Some of the genes in which their expression were differentially regulated at least twofold difference were further validated by qRT-PCR using total RNA isolated from a panel of ovarian cancer cell lines. For qRT-PCR, total RNA was treated by DNase I and then reverse transcribed with SuperScriptase II (Life Technologies). Generated cDNA was subjected to quantitative PCR with specific primer sets. The expression levels were standardized by comparing the Ct values of target to that of β-actin mRNA.

Intraperitoneal xenograft development assay

Intraperitoneal xenograft development was assessed as previously described.^{21,49} Briefly, cells in the log phase were trypsinized and resuspended in phosphate-buffered saline. Six-week-old athymic female nude mice (Hsd: athymic Nude-Foxn1nu, Harlan Sprague Dawley, Indianapolis, IN, USA) were intraperitoneally injected with 1×10^7 cells per mouse. To determine metastatic potential of ovarian cancer cells, mice were killed and autopsied 3 weeks after injection. Visible metastatic implants were collected and weighed. To determine the effect of AZD6244 and AZD0530 on metastatic colonization, mice were first injected with luciferase-expressing OVCAR3/Rac1G12V or SKOV3 cells for 12 days. AZD6244 and AZD0530 dissolved in 0.5% hydroxypropyl methylcellulose/0.1% Tween-80 were either alone or in combination administered orally to mice with the aid of gavages daily. Doses for AZD6244 and AZD0530 were 50 and 25 mg/kg, respectively. The controls were mice given with vehicle daily. Tumor progression was monitored by examining fluorescence in Xenogen IVIS-200 *In Vivo* Imaging System (Alameda, CA, USA) on weekly basis as previously described.⁵⁰ Visible implants in peritoneal cavities were harvested and fixed for immunohistochemistry. All procedures were approved by the Institution Animal Care Committee at Georgia Regents University.

Immunohistochemistry

Tumor tissues were collected immediately when tumor-bearing mice succumbed to death. Paraffin-embedded tissues were sectioned and subjected to immunohistochemistry to detect vimentin and E-cadherin using the respective antibodies as previously described.^{21,50}

Statistical analysis

Statistical analyses of *in vitro* invasion, cell shape change, cell migration, metastatic implant weights and gene expression levels were performed by analysis of variance and Student's *t*-test. Log-rank test was used to analyze the significance in mouse survival. Statistical analyses were aided by SPSS (release 15.0; SPSS Inc., IBM, North Castle, NY, USA). $P < 0.05$ was considered to be significant.

CONFLICT OF INTEREST

The authors declare no conflict of interest.

ACKNOWLEDGEMENTS

This work was supported by E-Institutes of Shanghai Municipal Education Commission (Project E03008), '085' First-Class Discipline Construction Innovation Science and Technology Support Project of Shanghai University of TCM (085ZY1206), National Science Foundation of China (31229002), NIH CA 187152 and DoD OC120313 (W81XWH-13-1-0122).

REFERENCES

- Jayson GC, Kohn EC, Kitchener HC, Ledermann JA. Ovarian cancer. *Lancet* 2014; **384**: 1376–1388.
- Seward SM, Winer I. Primary debulking surgery and neoadjuvant chemotherapy in the treatment of advanced epithelial ovarian carcinoma. *Cancer Metastasis Rev* 2015; **34**: 5–10.
- Thiery JP, Sleeman JP. Complex networks orchestrate epithelial-mesenchymal transitions. *Nat Rev Mol Cell Biol*. 2006; **7**: 131–142.
- Thiery JP. Epithelial-mesenchymal transitions in tumour progression. *Nat Rev Cancer* 2002; **2**: 442–454.
- Thiery JP, Acloque H, Huang RY, Nieto MA. Epithelial-mesenchymal transitions in development and disease. *Cell* 2009; **139**: 871–890.
- Lester RD, Jo M, Montel V, Takimoto S, Gonias SL. uPAR induces epithelial-mesenchymal transition in hypoxic breast cancer cells. *J Cell Biol* 2007; **178**: 425–436.
- Yang MH, Wu MZ, Chiou SH, Chen PM, Chang SY, Liu CJ et al. Direct regulation of TWIST by HIF-1 α promotes metastasis. *Nat Cell Biol* 2008; **10**: 295–305.
- Wu Y, Deng J, Rychahou PG, Qiu S, Evers BM, Zhou BP. Stabilization of snail by NF- κ B is required for inflammation-induced cell migration and invasion. *Cancer Cell* 2009; **15**: 416–428.
- Lopez-Novoa JM, Nieto MA. Inflammation and EMT: an alliance towards organ fibrosis and cancer progression. *EMBO Mol Med* 2009; **1**: 303–314.

- Prasanphanich AF, Arencibia CA, Kemp ML. Redox processes inform multivariate transdifferentiation trajectories associated with TGF β -induced epithelial-mesenchymal transition. *Free Radic Biol Med* 2014; **76**: 1–13.
- Davidson B, Trope CG, Reich R. Epithelial-mesenchymal transition in ovarian carcinoma. *Front Oncol* 2012; **2**: 33.
- Huang RY, Chung VY, Thiery JP. Targeting pathways contributing to epithelial-mesenchymal transition (EMT) in epithelial ovarian cancer. *Curr Drug Targets* 2012; **13**: 1649–1653.
- Takai M, Terai Y, Kawaguchi H, Ashihara K, Fujiwara S, Tanaka T et al. The EMT (epithelial-mesenchymal-transition)-related protein expression indicates the metastatic status and prognosis in patients with ovarian cancer. *J Ovarian Res* 2014; **7**: 76.
- Davidson B, Holth A, Helleslyt E, Tan TZ, Huang RY, Trope C et al. The clinical role of epithelial-mesenchymal transition and stem cell markers in advanced-stage ovarian serous carcinoma effusions. *Hum Pathol* 2015; **46**: 1–8.
- Cancer Genome Atlas Research Network. Integrated genomic analyses of ovarian carcinoma. *Nature* 2011; **474**: 609–615.
- Yoshida S, Furukawa N, Haruta S, Tanase Y, Kanayama S, Noguchi T et al. Expression profiles of genes involved in poor prognosis of epithelial ovarian carcinoma: a review. *Int J Gynecol Cancer* 2009; **19**: 992–997.
- Tan TZ, Miow QH, Miki Y, Noda T, Mori S, Huang RY et al. Epithelial-mesenchymal transition spectrum quantification and its efficacy in deciphering survival and drug responses of cancer patients. *EMBO Mol Med* 2014; **6**: 1279–1293.
- Ponnusamy MP, Lakshmanan I, Jain M, Das S, Chakraborty S, Dey P et al. MUC4 mucin-induced epithelial to mesenchymal transition: a novel mechanism for metastasis of human ovarian cancer cells. *Oncogene* 2010; **29**: 5741–5754.
- Chen D, Zhang Y, Wang J, Chen J, Yang C, Cai K et al. MicroRNA-200c over-expression inhibits tumorigenicity and metastasis of CD117+CD44+ ovarian cancer stem cells by regulating epithelial-mesenchymal transition. *J Ovarian Res* 2013; **6**: 50.
- Ahmed N, Abubaker K, Findlay J, Quinn M. Epithelial mesenchymal transition and cancer stem cell-like phenotypes facilitate chemoresistance in recurrent ovarian cancer. *Curr Cancer Drug Targets* 2010; **10**: 268–278.
- Chen H, Wu X, Pan ZK, Huang S. Integrity of SOS1/EP8/ABL1 tri-complex determines ovarian cancer metastasis. *Cancer Res* 2010; **70**: 9979–9990.
- Yamada SD, Hickson JA, Hrobowski Y, Vander Griend DJ, Benson D, Montag A et al. Mitogen-activated protein kinase kinase 4 (MKK4) acts as a metastasis suppressor gene in human ovarian carcinoma. *Cancer Res* 2002; **62**: 6717–6723.
- Scita G, Nordstrom J, Carbone R, Tenca P, Giardina G, Gutkind S et al. EP8 and E3B1 transduce signals from Ras to Rac. *Nature* 1999; **401**: 290–293.
- Moustakas A, Heldin CH. Induction of epithelial-mesenchymal transition by transforming growth factor beta. *Semin Cancer Biol* 2012; **22**: 446–454.
- Parvani JG, Taylor MA, Schiemann WP. Noncanonical TGF- β signaling during mammary tumorigenesis. *J Mammary Gland Biol Neoplasia* 2011; **16**: 127–146.
- Brabletz S, Bajdak K, Meidhof S, Burk U, Niedermann G, Firat E et al. The ZEB1/miR-200 feedback loop controls Notch signalling in cancer cells. *EMBO J* 2011; **30**: 770–782.
- Wu Y, Ginther C, Kim J, Mosher N, Chung S, Slamon D et al. Expression of Wnt3 activates Wnt/ β -catenin pathway and promotes EMT-like phenotype in trastuzumab-resistant HER2-overexpressing breast cancer cells. *Mol Cancer Res* 2012; **10**: 1597–1606.
- Lu Z, Ghosh S, Wang Z, Hunter T. Downregulation of caveolin-1 function by EGF leads to the loss of E-cadherin, increased transcriptional activity of β -catenin, and enhanced tumor cell invasion. *Cancer Cell* 2003; **4**: 499–515.
- Radisky DC, Bissell MJ. NF- κ B links oestrogen receptor signalling and EMT. *Nat Cell Biol* 2007; **9**: 361–363.
- Cichon MA, Radisky DC. ROS-induced epithelial-mesenchymal transition in mammary epithelial cells is mediated by NF- κ B-dependent activation of Snail. *Oncotarget* 2014; **5**: 2827–2838.
- Tian L, Li L, Xing W, Li R, Pei C, Dong X et al. IRGM1 enhances B16 melanoma cell metastasis through PI3K-Rac1 mediated epithelial mesenchymal transition. *Sci Rep* 2015; **5**: 12357.
- Zhang Z, Yang M, Chen R, Su W, Li P, Chen S et al. IBP regulates epithelial-to-mesenchymal transition and the motility of breast cancer cells via Rac1, RhoA and Cdc42 signaling pathways. *Oncogene* 2014; **33**: 3374–3382.
- Yang WH, Lan HY, Huang CH, Tai SK, Tzeng CH, Kao SY et al. RAC1 activation mediates Twist1-induced cancer cell migration. *Nat Cell Biol* 2012; **14**: 366–374.
- Leng R, Liao G, Wang H, Kuang J, Tang L. Rac1 expression in epithelial ovarian cancer: effect on cell EMT and clinical outcome. *Med Oncol* 2015; **32**: 329.
- Theriault BL, Shepherd TG, Mujoomdar ML, Nachtigal MW. BMP4 induces EMT and Rho GTPase activation in human ovarian cancer cells. *Carcinogenesis* 2007; **28**: 1153–1162.
- McGrail DJ, Kieu QM, Dawson MR. The malignancy of metastatic ovarian cancer cells is increased on soft matrices through a mechanosensitive Rho-ROCK pathway. *J Cell Sci* 2014; **127**(Pt 12): 2621–2626.

- 37 Gou WF, Zhao Y, Lu H, Yang XF, Xiu YL, Zhao S *et al*. The role of RhoC in epithelial-to-mesenchymal transition of ovarian carcinoma cells. *BMC Cancer* 2014; **14**: 477.
- 38 Huang RY, Wong MK, Tan TZ, Kuay KT, Ng AH, Chung VY *et al*. An EMT spectrum defines an anoikis-resistant and spheroidogenic intermediate mesenchymal state that is sensitive to e-cadherin restoration by a src-kinase inhibitor, saracatinib (AZD0530). *Cell Death Dis* 2013; **4**: e915.
- 39 Condello S, Cao L, Matei D. Tissue transglutaminase regulates beta-catenin signaling through a c-Src-dependent mechanism. *FASEB J* 2013; **27**: 3100–3112.
- 40 Cheng S, Guo J, Yang Q, Yang X. Crk-like adapter protein regulates CCL19/CCR7-mediated epithelial-to-mesenchymal transition via ERK signaling pathway in epithelial ovarian carcinomas. *Med Oncol* 2015; **32**: 47.
- 41 Javle MM, Gibbs JF, Iwata KK, Pak Y, Rutledge P, Yu J *et al*. Epithelial-mesenchymal transition (EMT) and activated extracellular signal-regulated kinase (p-Erk) in surgically resected pancreatic cancer. *Ann Surg Oncol* 2007; **14**: 3527–3533.
- 42 Mandal M, Myers JN, Lippman SM, Johnson FM, Williams MD, Rayala S *et al*. Epithelial to mesenchymal transition in head and neck squamous carcinoma: association of Src activation with E-cadherin down-regulation, vimentin expression, and aggressive tumor features. *Cancer* 2008; **112**: 2088–2100.
- 43 Bid HK, Roberts RD, Manchanda PK, Houghton PJ. RAC1: an emerging therapeutic option for targeting cancer angiogenesis and metastasis. *Mol Cancer Ther* 2013; **12**: 1925–1934.
- 44 Chen H, Zhu G, Li Y, Padia RN, Dong Z, Pan ZK *et al*. Extracellular signal-regulated kinase signaling pathway regulates breast cancer cell migration by maintaining slug expression. *Cancer Res* 2009; **69**: 9228–9235.
- 45 Hong S, Noh H, Teng Y, Shao J, Rehmani H, Ding HF *et al*. SHOX2 is a direct miR-375 target and a novel epithelial-to-mesenchymal transition inducer in breast cancer cells. *Neoplasia* 2014; **16**: 279–90 e5.
- 46 Li Y, Zhang M, Chen H, Dong Z, Ganapathy V, Thangaraju M *et al*. Ratio of miR-196s to HOXC8 messenger RNA correlates with breast cancer cell migration and metastasis. *Cancer Res* 2010; **70**: 7894–7904.
- 47 Li Y, Guo Z, Chen H, Dong Z, Ding H, Huang S. HOXC8-dependent cadherin 11 expression facilitates breast cancer cell migration through Trio and Rac. *Genes Cancer* 2012; **2**: 880–888.
- 48 Li Y, Chao F, Huang B, Liu D, Kim J, Huang S. HOXC8 promotes breast tumorigenesis by transcriptionally facilitating cadherin-11 expression. *Oncotarget* 2014; **5**: 2596–2607.
- 49 Yang L, Fang D, Chen H, Lu Y, Dong Z, Ding HF *et al*. Cyclin-dependent kinase 2 is an ideal target for ovary tumors with elevated cyclin E1 expression. *Oncotarget* 2015; **6**: 20801–20812.
- 50 Hu Q, Lu YY, Noh H, Hong S, Dong Z, Ding HF *et al*. Interleukin enhancer-binding factor 3 promotes breast tumor progression by regulating sustained urokinase-type plasminogen activator expression. *Oncogene* 2013; **32**: 3933–3943.

Supplementary Information accompanies this paper on the Oncogene website (<http://www.nature.com/onc>)